V. PHENOMENOLOGY AND THE CONSTITUENT INTERCHANGE MODEL

In Sections I and IV we have described the hard scattering models and their properties from a fairly general viewpoint. In order to discuss specific calculations, we now turn to constituent interchange model which provides a definite dynamical realization of a quark parton model for hadronic reactions, and in which all of the generalized properties outlined in Section ID are explicitly fulfilled. These include the exclusive-inclusive connection, generalized Regge behavior, and the dimensional counting rules. From one point of view the CIM provides a covariant, but simple procedure for calculating the dynamics of duality diagrams at large momentum transfer, and thus it naturally incorporates the quark degrees of freedom of hadrons. On the other hand it is compatible with the conventional Regge and completely hadronic descriptions of low-momentum-transfer processes. Detailed discussions of the CIM may be found in the varied papers of Blankenbecler, Brodsky, Gunion, and Savit (1972-1975) and Landshoff and Polkinghorne (1973, 1974). Further calculational details are discussed by Fishbane and Muzinich (1973), and M. Schmidt (1974). An introduction to calculational methods is given in Appendix B. An early comparison of calculation methods and applications of the covariant parton model and the CIM can be found in lectures of Polkinghorne (1972) and Blankenbecler (1972).

A. The Structure of the CIM

The physical structure of the CIM for both exclusive and inclusive processes at large momentum transfer is shown schematically in Fig. VA. 1. The model begins with a basic irreducible large-angle subprocess a+b → c+d, involving quarks plus states with hadronic quantum numbers, which is then weighted by the covariant amplitudes for the fragmentation or formation of the scattering hadrons. Thus, inclusive processes at large t and u are controlled by quark-hadron scattering, and exclusive processes always involves quark interchange or quark exchange. We have already discussed in Section IVC why scale-invariant quark-quark scattering involving quarks of different hadrons seems to be negligible or absent. The hypothesis that quark exchange processes should be dominate was originally made (Blankenbecler et al., 1972) to account for the difference in normalization of large angle $pp \to pp$ and $p\bar{p} \to p\bar{p}$ processes, and the fact that it accounts well for the angular structure of the exclusive processes, especially $K^+p \to K^+p$, and $pp \to pp$. However, unless it is suppressed by kinematics, one must allow for hadronic radiation or bremsstrahlung from the initial beam particles A and B. Thus bremsstrahlung is analogous to the real and virtual radiative corrections to electromagnetic reactions and it "dresses" and reggeizes the hadronic processes. In the case of real hadronic bremsstrahlung, the effects may be incorporated into the $x \to 0$ behavior of the structure function $G_{a/A}(x)$ and $G_{b/B}(x)$, which is related to the Regge behavior of the cross sections $\sigma_{\bar{a}A}$ and $\sigma_{\bar{b}B}$ (see Section IV). In the case of virtual bremsstrahlung, the coherent emission and absorption of hadrons between particles A and C moves the Regge poles $\alpha_{AC}(t)$ away from their asymptotic values at large t. This is discussed in detail by Blankenbecler, Brodsky, Gunion, and Savit (1973). The virtual radiation can be neglected at large t and u, thus

exposing the minimal "impulse approximation" terms which yield power law scaling laws at fixed angle. There is also the possibility of absorption corrections from Pomeron exchanges of the initial particles, which is controlled asymptotically by the S-matrix at zero impact parameter (see Blankenbecler et al., 1972; Kane, 1974). Absorptive corrections are assumed to not change the asymptotic scaling laws, but there can be residual effects reflecting the geometrical sizes of hadrons at moderate t values. The small oscillating structure in pp → pp scattering (see Fig. IIA.7) observed as a function of t by Hendry (1974) and discussed by Shrempp and Shrempp (1974) is thus not necessarily in conflict with the asymptotic validity of parton model ideas.

In order to examine the structure of the CIM, let us first consider the inclusive reactions A+B → C+X in a region of phase space where bremsstrahlung from particles A and C should be suppressed, for example, the "triple-Regge" region where $\mathcal{M}^2 \ll s$, and $s >> -t$, but $|t|$ is still large. The leading CIM contribution is then quark-hadron scattering q+A → q+C, on the quarks of the target particle B. An elementary calculation, which parallels the standard parton model calculations for deep inelastic lepton scattering term gives (see Fig. VA.1a)

$$E\frac{d\sigma}{d^3p} \cong \frac{1}{\pi}\sum_q \frac{s}{s+u}\; x\, G_{q/B}(x)\,\frac{d\sigma}{dt}(Aq \to Cq)\Big|_{\substack{s'=xs\\ t'=t\\ u'=xu}} \qquad \text{(VA.1)}$$

where $x = -t/(s+u) = -t/(\mathcal{M}^2 - t)$, is the familiar Bjorken scaling variable. The assumptions here include the convergence of the transverse momentum integrations (i.e., the existence of the $G_{q/B}(x)$), and incoherence of the various quark contributions, and the usual neglect of the quark confinement problem.

There exists a corresponding contribution to the exclusive amplitude $A+B \to C+D$ calculated according to Fig. VA.1c. In this case an integral over the fractional momentum (or light-cone variable) $x = (k_0+k_3)/(p_0+p_3)$ variable is required. Using the mean value theorem we can write the contribution from scattering on one quark

$$\frac{d\sigma}{dt}(A+B \to C+D) \cong F^2_{BD}(t) \frac{d\sigma}{dt}(Aq \to C+q)\Big|_{\substack{s'=\bar{x}s \\ t'=t}} , \qquad \text{(VA.2)}$$

although in fact here the quark contributions should add coherently. The central assumption in Eq. (VA.2) is that the vertex function of particles B and D converge most rapidly; in general the integral gives additional contributions where hadrons A, C, or D are treated as the target. The value of $\bar{x}$ is obtained from the mean value theorem. In practical cases $\bar{x}$ gives the dominant region of integration when $\bar{x}$ is near q. The form factor $F_{BD}(t)$ falls at the same rate as the elastic form factor.

The expression (VA.1) and (VA.2) have simple analogues when we treat the coherent and incoherent scattering the nucleons of a nuclear target; the function G(x) is given by the Fermi distribution, and $F_{BD}(t)$ is the body form factor of a nucleon in the nucleus. In the case of lepton scattering (VA.1) and (VA.2) are the standard parton model results. In the case of photon-scattering, (VA.2) predicts the dominance of J=0 fixed pole behavior of the Compton amplitude $\gamma p \to \gamma p$ at large t, and fixed pole behavior at J below 1 for meson photoproduction.

As in Section ID, we see that the inclusive and exclusive scattering cross sections are connected and join smoothly since they have the same behavior on the kinematic variables in this limit. A calculation of the relative normalization is difficult. One difficulty is that of simply computing the inclusive cross section at a small missing mass, and another arises from the fact that the simple incoherent sum over final states used above is not justified since many of the final states become coherent at small missing mass. Therefore, one should not expect the theoretical formulas to lead to a smoother connection than expected from the above discussion. We also see that this connection will hold both at fixed t and at fixed scattering angle.

LIST OF FIGURES FOR SECTION VA

STRUCTURE OF THE C.I.M.

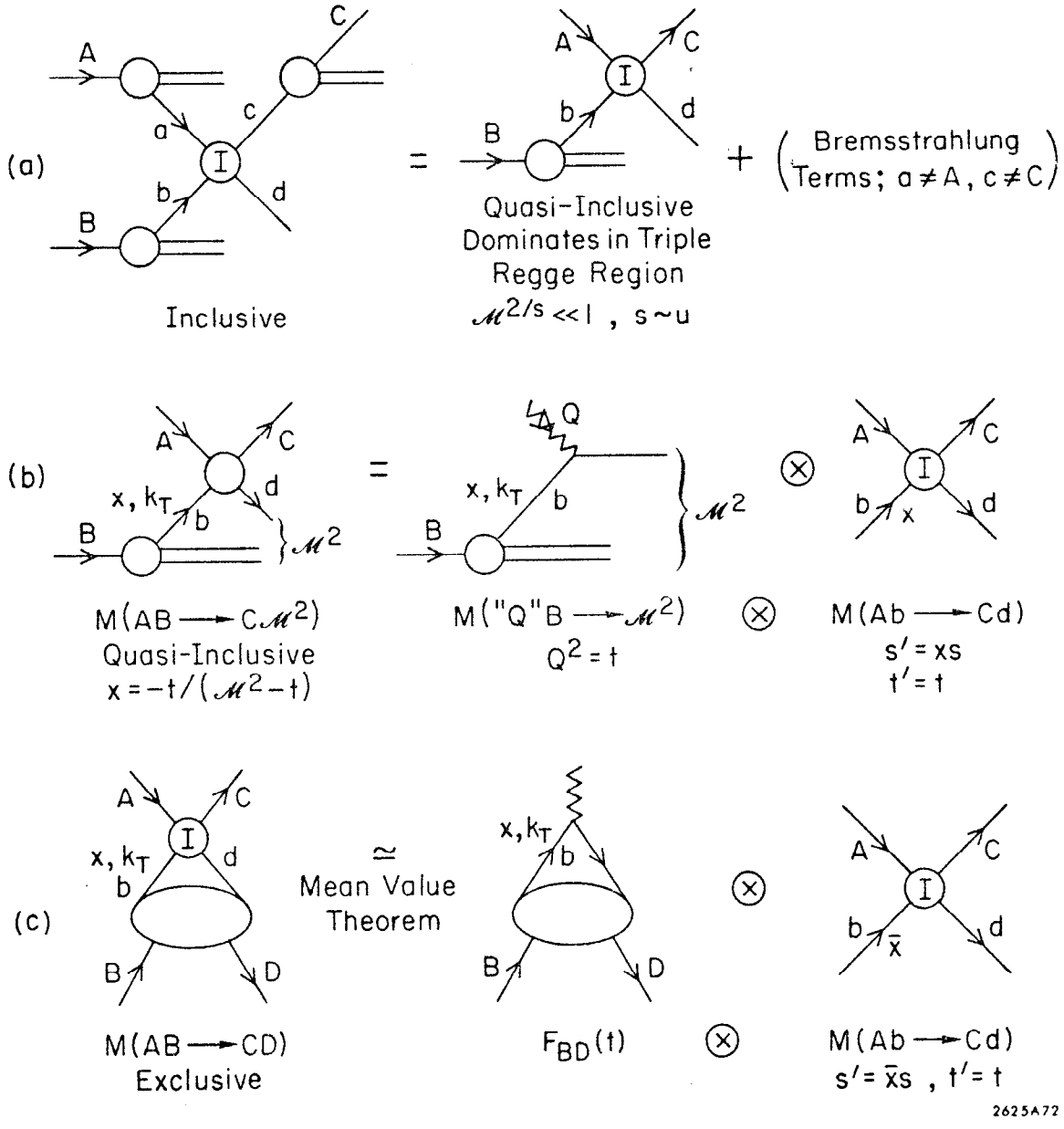

FIG. VA.1

B. Inclusive Scattering in the CIM

Triple Regge Region

Let us now examine the triple Regge region by including the Regge effects just discussed. We now have for the basic scattering of a quark and a hadron

$$\frac{d\sigma}{dt}(Aq \to Cq) = \left|\gamma(t')(-u')^{\alpha_{AC}(t')} + \tilde{\gamma}(t')(-s)^{\alpha_{AC}(t')}\right|^2/s^2 \qquad \text{(VB.1)}$$

$\gamma(-\infty)$ = constant, and $\alpha_{AC}(-\infty)$ is given by the counting rules. Both terms are needed to get the angular distribution correct and the inclusive cross section arising from this basic process becomes

$$\frac{Ed\sigma}{d^3p} = \frac{x_1^2}{\left(p_T^2+m^2\right)^{2-2\alpha(t)}} x G_{q/B}(x)\left[\frac{\mathcal{M}^2-t}{s}\right]^{1-2\alpha(t)} \left|\gamma(t)+\tilde{\gamma}(t)(-x_1)^{-\alpha(t)}\right|^2 + \ldots \qquad \text{(VB.2)}$$

Now one can identify the expected triple Regge behavior and corrections to it when $x_1 \neq 1$ and $x \neq 0$.

Central Region

In order to get particles into the central region, it is advantageous to let both incident particles A and B bremsstrahlung, lose momentum and collide at a low relative effective energy. This type of inclusive process is conveniently decomposed into peripheral interactions, hadronic bremsstrahlung and the basic irreducible process as illustrated in Fig. VA.1. A very large class of theories including many of the statistical models can also be decomposed in this fashion. The resulting cross section is of the form (given in Eq. (IC.10))

$$\frac{Ed\sigma}{d^3p}(A+B \to C+X) = \sum_{a,b}\int dx\, dy\; G_{a/A}(x)\, G_{b/B}(y)\, \frac{Ed\sigma^I}{d^3p}(a+b \to C+d^*)\Big|_{\substack{s'=xys \\ t'=xt \\ u'=yu}} \qquad \text{(VB.3)}$$

and

$$M_a^2 + M_b^2 + M_C^2 + M_{d^*}^2 = xys + xt + yu \quad .$$

The possibility of bremsstrahlung from the final state C will be discussed shortly.

The irreducible process $a+b \to C+d^*$ (no extra hadrons are allowed to be emitted) can be conveniently separated into contributing graphs as depicted in Fig. VB.1. The first term on the right is the pure fixed power behaved amplitudes previously discussed while the second term gives rise to Regge behavior for the process $a+q \to C+q$. The third term corresponds to the production of a state c in the basic interaction that subsequently decays to the observed particle C.

Using the relation between the irreducible and total probability functions

$$G_{q/B}(x) = \int_x^1 \frac{dz}{z} \sum_b G^I_{q/b}\left(\frac{x}{z}\right) G_{b/B}(z) \quad , \qquad \text{(VB.4)}$$

the inclusive cross section can be written in the convenient but unsymmetrical form

$$\frac{E d\sigma}{d^3p}(A+B \to C+X) = \int_{z_c}^1 dz \sum_a G_{a/A}(z) \frac{E d\sigma}{d^3p}(a+B \to C+X) \quad , \qquad \text{(VB.5)}$$

where $z_0 = -u/(s+t)$ and the inclusive cross section under the integral is evaluated at $s' = zs$, $u' = u$, and $t' = zt$. Recall that in this formula, small intermediate transverse momenta have been neglected, and the required symmetrization between the particles has not been explicitly denoted. This is easily handled in any specific reaction of interest.

The general behavior of the inclusive cross section can be understood from quite simple kinematic arguments that are of course implicitly contained in the

above formula. The basic (internal) process is $a+q \rightarrow C+q$ and it has an $(\text{energy})^2$ of

$$s_{eff} = xys \sim \frac{x^2(-u)s}{xs+t} \geq 4p_T^2 \quad , \tag{VB.6}$$

if the missing mass M_{d^*} is kept finite. Therefore this process is operating at a fixed angle and at an $s_{eff} \sim 4p_T^2$, and one expects the cross section to fall as $\left(p_T^2\right)^{-N}$, where N is related to the total number of constituents involved in this subreaction. Thus the p_T dependence of the inclusive cross section is related to and determined by the number of constituents involved in the basic process.

Let us further examine the central region where $p_T^2 = tu/s \cong$ constant, and $\epsilon = \mathcal{M}^2/s \cong 1$. The integral over z is easily estimated in the above formula and one finds

$$\frac{Ed\sigma}{d^3p} = \sum_a G_a(x_L, \epsilon) \left(p_T^2\right)^{-N_a} \tag{VB.7}$$

where $N_a \equiv 2\left(1 - \alpha_{aC}(<z> t)\right)$, and $<z>$ is the average value of z involved in the integral. For large $|t|$, $\alpha_{aC} \approx \alpha_{aC}(-\infty)$ which is a number determined by counting. For example, $\alpha_{aC} = -1$ yields p_T^{-8} terms, $\alpha_{aC} = -2$ yields p_T^{-12} terms, etc. The p_T dependence reflects the fixed angle behavior of the basic process $a+b \rightarrow C+d^*$ of course.

A second interesting region is the threshold region defined by $\epsilon \rightarrow 0$. This limit should suppress the bremsstrahlung contributions and one finds that this is indeed the case. Note that the suppression works from both ends of the integral since $z_0 = 1 - \epsilon/(1+t/s) \rightarrow 1$, and also, the x variable in the inclusive process under the integral is

$$x' = -\frac{t'}{s'+u'} = \frac{(z-z_0)(s+t)}{(zs+u)} \quad . \tag{VB.8}$$

Thus in the integrand, $z \sim z_0$ is suppressed and of course $z \sim 1$ is suppressed by the explicit G(z) probability function. One finds

$$\frac{E d\sigma}{d^3p} \cong \sum_{a,b} \epsilon^{F(a,b)} \gamma_{ab}(p_T, u/s) \qquad \text{(VB.9)}$$

where

$$F(a,b) = g(a/A) + g(b/B) + 1 \quad . \qquad \text{(VB.10)}$$

Let us now examine the integral in more detail for a general contribution. We will assume that argument of $\alpha(t')$ can be replaced by a constant under the integral, that is $t' \to \langle t' \rangle = -2p_T^2 (1+\langle z \rangle)^{-1}$, and assume the probability functions have the simple form $G(x) \propto (1-x)^g/x$. Finally, the basic cross section will be written in the general form

$$\frac{d\sigma}{dt}(s,z) \propto (s' + m^2)^{-N} \left(\frac{1-z}{2}\right)^{-b} \left(\frac{1+z}{2}\right)^{-a} \qquad \text{(VB.11)}$$

where N, a and b may depend parametrically on p_T^2 through their dependence on $\alpha(t')$, since $N \equiv 2 - 2\alpha(\langle t' \rangle) + b$.

The integral for the inclusive cross section is

$$\frac{E d\sigma}{d^3p} \propto \int_{-(1-2x_1)}^{(1-2x_2)} \frac{dz}{(1-z^2)} \left(1 - \frac{2x_1}{1+z}\right)^{g_A} \left(1 - \frac{2x_2}{1-z}\right)^{g_B} \left(\frac{1-z^2}{4p_T^2}\right)^N \left(\frac{1-z}{2}\right)^{-b} \left(\frac{1+z}{2}\right)^{-a} \qquad \text{(VB.12)}$$

where $x_1 = -u/s$, $x_2 = -t/s$. Changing variables, this can be written as

$$\frac{E d^3\sigma}{d^3p} = \frac{\epsilon^F f_0}{2\left(p_T^2 + M^2\right)^N} I(x_1, x_2)$$

where $M^2 \cong m^2(1-\langle z \rangle)/4$, $\epsilon = 1 - x_1 - x_2$, and

$$I(x_1, x_2) = \int_0^1 d\eta\, \eta^{g_A} (1-\eta)^{g_B} \left(x_2 + \epsilon(1-\eta)\right)^{N-1-g_B-b} \left(x_1 + \epsilon\eta\right)^{N-1-g_a-a} \qquad \text{(VB.13)}$$

This integral representation has several advantages. It explicitly shows the basic symmetry of the result in $x_1 \leftrightarrow x_2$ if $g_B \leftrightarrow g_A$ and $a \leftrightarrow b$. It is also in the form of the integral representation for a hypergeometric function of two variables (Bateman, HTF, Vol. 1, p. 231). The associated reduction and transformation formulae are very convenient in extracting the limiting behavior of $I(x_1 x_2)$ in a variety of regions (Pearson, 1974). For example, in the singular limit of g_A or $g_B \to -1$, the integration is dominated by an endpoint behavior and one recovers the expected triple Regge formula. If the probability functions vanish at x=0, extra powers of x_1 and/or x_2 occur outside the integral $I(x_1, x_2)$.

Note that if $\epsilon \to 0$ for finite x_1 and x_2, the cross section vanishes as ϵ^F. However, in the triple Regge region, where $1 \cong x_1 >> \epsilon >> x_2$, I is easily shown to behave as ϵ^{N-1-g_B-b}. This result can be interpreted as a triple Regge formula with an effective trajectory given by

$$\alpha_{eff}(t) = \alpha_{AC}(<t'>) - \frac{1}{2}(1 + g(a/A)) \qquad \text{(VB.14)}$$

which can be identified as a nonleading disconnected cut contribution.

We have now identified a second important correction to the triple Regge formula which should become important at large missing mass and provides the correct extrapolation into the central region. An analysis of reactions of the form $pp \to CX$, where $C = p, \pi^{\pm}, K^{\pm}, \bar{p}$, has been carried out by Chen, Wang, and Wong (1972). As discussed in more detail by Blankenbecler and Brodsky (1974), their results for the effective trajectory provide evidence for the type of correction we are discussing and for the quantum number dependence predicted by the above formula for α_{eff}.

In the preceding discussion, the possibility that the particle C observed at large p_T arose from the decay of a state, say c, which was produced at large p_T, was not included. We have already argued that a basic large angle scattering process produces resonances with roughly the same cross section as particles, and therefore it is important to take this into account. Generalizing the formula to this case, it is clear one has (see Appendix A)

$$\frac{E d\sigma}{d^3p} = \sum_{a,b,c} \int dx\, dy\, dz\; G_{a/A}(x)\, G_{b/B}(y)\, \tilde{G}_{C/c}\left(\frac{1}{z}\right) \frac{d\sigma}{dt}(ab \to cd^*)\Big|_{\substack{s'=xys \\ t'=zxt \\ u'=zyu}}$$

$$\frac{xys}{\pi}\, \delta(xys + zxt + zyu) \qquad \text{(VB.15)}$$

Since particle c must have more momentum than the detected one, C, the argument of $\tilde{G}_{C/c}$ is 1/z, where 1/z is between 0 and 1. Using similar arguments as before, the threshold behavior of the cross section is given by $F = 2(n(\bar{a}A) + n(\bar{b}B) + n(\bar{c}C)) - 1$ and the p_T^2 power N depends on the basic process just as before.

Roth (1974) has emphasized that since $(sEd\sigma/d^3p)$ arises from the discontinuity of a $3 \to 3$ amplitude, the same amplitude should describe the two processes $A+B \to C+X$ and $\bar{C}+B \to \bar{A}+X$, and they are connected by $s \leftrightarrow u$ crossing. Not all models will possess this property. In particular, those models that try to combine an exponential (statistical) final decay distribution with a power law initial state scattering amplitude cannot satisfy it.

This crossing relation must be satisfied and it leads to restrictions on the probability functions G(z). In particular, from the structure of the above equation there must exist a relation between G(z) and $\tilde{G}(1/z)$, and this relation for

scalar particles turns out to be

$$G_{a/A}(z) = -z\, \tilde{G}_{\bar{A}/\bar{a}}\left(\frac{1}{z}\right) \tag{VB.16}$$

If this relation is used for both $G_{a/A}$ and $\tilde{G}_{C/c}$, and one writes

$$\frac{d\sigma}{dt}(ab \to cd^*) = \frac{1}{s^2} |M(ab \to cd^*)|^2 \tag{VB.17}$$

one can easily cross this relation ($s \leftrightarrow u$) and arrive at the formula

$$\frac{E d\bar{\sigma}}{dt} = \sum_{ab,\,c} \int dz\, dy\, dx\, G_{\bar{c}/\bar{C}}(z)\, G_{b/B}(y)\, \tilde{G}_{\bar{A}/\bar{a}}\left(\frac{1}{x}\right) \frac{d\sigma}{dt}(\bar{c}b \to \bar{a}d^*)$$

$$\frac{xys}{\pi}\, \delta(zys + zxt + xyu) \tag{VB.18}$$

which is of the same form as the original equation.

This continuation formula for G is consistent with the integral equation satisfied by the G's. That is, if the hadron irreducible function G^I satisfies this relation, then so does the full G. Writing Eq. (VB.4) in the form

$$-z\, G_{B/A}\left(\frac{1}{z}\right) = -z \sum_a \int_{1/z}^{1} \frac{dx}{x} G^I_{B/a}\left(\frac{1}{xz}\right) G_{a/A}(x) \tag{VB.19}$$

and using the continuation formula twice on the right hand side and the change of variable $xz \to x$, one finds

$$-z\, G_{B/A}\left(\frac{1}{z}\right) = \sum_a \int_z^1 \frac{dx}{x}\, \tilde{G}^I_{\bar{A}/\bar{a}}\left(\frac{z}{x}\right) \tilde{G}^I_{\bar{a}/\bar{B}}(x) \quad \tilde{G}_{\bar{A}/\bar{B}}(z) \tag{VB.20}$$

as required, since $\tilde{G}$ satisfies the conjugate equation to (VB.4).

It is amusing to note that a general solution of this functional equation, if one requires that $G_{B/A} = G_{A/B} = G_{\bar{A}/\bar{B}}$, is

$$G(x) = \frac{1-x}{x}\,(1 + x^2 - ax)\, g\left(\frac{1}{x} + x\right) \tag{VB.21}$$

If a=2 and g = constant, this reduces to a commonly used approximate form for the nucleon's structure function. If spin one-half particles are involved, there is an extra factor of $(-1)^{f(A,B)}$, where $f^{(A,B)}$ is the total number of fermions in the state $(\bar{A}B)$. This factor arises from the associated spin traces; its effects need to be fully explored in the general case.

LIST OF FIGURES FOR SECTION VB

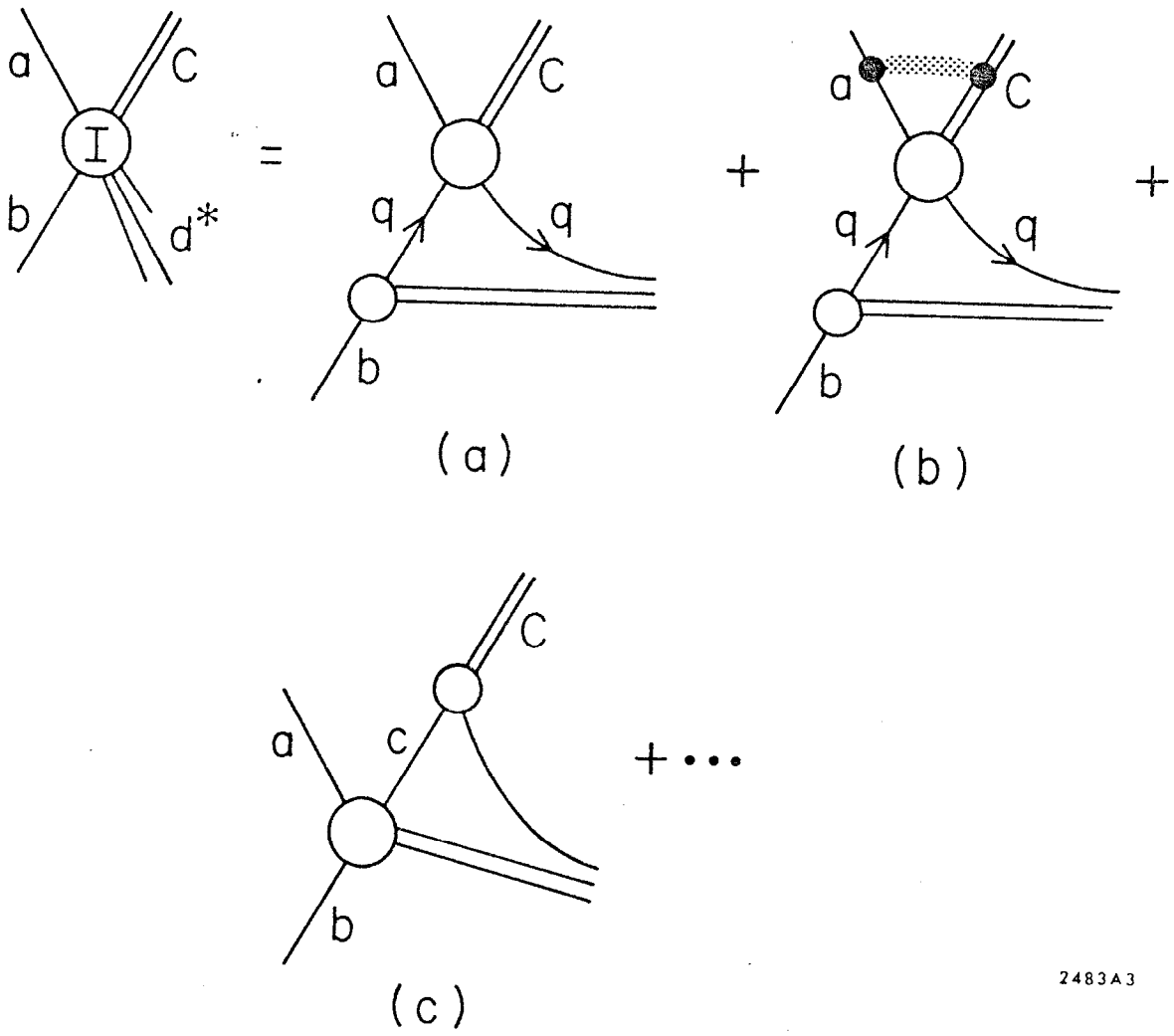

FIG. VB.1

C. Exclusive Scattering in the Constituent Interchange Model

The objective of this section is to discuss several exclusive scattering processes and to extract their expected angular as well as energy dependences in the CIM. This will lead naturally into a discussion of the connection between the fixed angle and fixed t (Regge) behavior. As we shall see, this type of composite model predicts a particularly simple connection which has many experimental ramifications. A discussion of calculations of the scattering of composite systems is given in Appendix C.

The crucial result which characterizes a scattering matrix element in the CIM is

$$M_{AB \to CD}(u,t) \sim F^q_{BD}(t)\, M_{qA \to qC}(u,t) + \ldots \qquad \text{(VC.1)}$$

where $F^q_{BD}(t)$ falls in t as the $B \to D$ transition form factor and q is a constituent of particle B as illustrated in Fig. VC.1a. The crossed diagram of VC.1b is also present. Direct quark-quark scattering such as in Fig. VC.1c is neglected.

Let us now apply this formula to meson-baryon scattering, first ignoring spin effects. In general, the scattering amplitude is a linear combination of (ut) and (st) contributions which we will write in the form

$$M(s,t,u) = \alpha\, M(u,t) + \beta\, M(s,t) \qquad \text{(VC.2)}$$

where asymptotically

$$M(u,t) \sim (-t)^{-2}\,(-u)^{-1} \qquad \text{(VC.3)}$$

for the constituent interchange diagram of Fig. VC.2b. The factor $(t)^{-2}$ is interpretable as a "form factor" of the nucleon as illustrated in Fig. VC.2a, while $(-u)^{-1}$ is the quark-pion scattering amplitude.

The value of α and β for a particular reaction depends upon the quantum numbers assigned to the constituents. R. Pearson (1974) has evaluated these

coefficients in the SU(3) quark model. He further separates the terms into contributions arising from a hadronic core having quantum numbers of a $\{6\}$ and a $\{\bar{3}\}$ by writing $\alpha = \alpha(6) + \alpha(\bar{3})$ and similarly for β. The values for a selected set of reactions is given in Table V.1. Once the behavior of the M's are given, the values of α and β determine the angular distribution at large angles. In the simple quark counting model, the core is $\{6\} + 3\{\bar{3}\}$. However, the inclusion of the effects of spin (see below) modifies the expected angular distributions without changing the energy dependence at fixed angle. Absorptive corrections are assumed to affect the magnitude of M but not its large angle behavior if the absorption is smooth at short distances (as suggested by Kane, 1974).

A specific model for meson-baryon scattering which included the effects of spin and assumed that the baryon was primarily a bound state of a quark and a spin one core was discussed by Blankenbecler, Brodsky and Gunion (1973). In this model, helicity is conserved asymptotically and the cross section has the form

$$\frac{d\sigma}{dt} \propto (-u/s)\,|B|^2 \qquad \text{(VC.3)}$$

with

$$B(s,t,u) = \alpha\, B(u,t) + \beta\, B(s,t) \qquad \text{(VC.4)}$$

where

$$B(u,t) \sim (-u)^{-2}\,(-t)^{-2} \qquad \text{(VC.5)}$$

for $|u|$ and $|t|$ large. Predictions for some typical differential cross sections in the limit of exact SU(3) are given in Table V.2. See also Fig. VC.3.

The above invariant matrix element can also be used to describe the annihilation of $\bar{p}p$ into mesons by continuing to this channel by $s \leftrightarrow t$ crossing. Two

TABLE V.1

Reaction	$\alpha(6)$	$\alpha(\bar{3})$	$\beta(6)$	$\beta(\bar{3})$
$\pi^+ p \to \pi^+ p$	1	1	2	0
$\pi^- p \to \pi^- p$	2	0	1	1
$\pi^- p \to \pi^0 n$	$-1/\sqrt{2}$	$1/\sqrt{2}$	$1/\sqrt{2}$	$-1/\sqrt{2}$
$K^+ p \to K^+ p$	1	1	0	0
$K^- p \to K^- p$	0	0	1	1
$K_L p \to K_S p$	-1	0	1	0
$\pi^+ p \to K^+ \Sigma^+$	0	0	-2	0
$K^- p \to \eta \Sigma^0$	$-1/\sqrt{3}$	0	$1/\sqrt{3}$	0

TABLE V.2

$$\frac{d\sigma}{dt} \equiv \frac{\sigma_0}{s^8} \frac{(1+z)}{(1-z)^4} R^2(z)$$

Reaction	R(z)
$\pi^+ p \rightarrow \pi^+ p$	$4\alpha(1+z)^{-2} + \beta$
$\pi^- p \rightarrow \pi^- p$	$4\beta(1+z)^{-2} + \alpha$
$K^+ p \rightarrow K^+ p$	$4\alpha(1+z)^{-2}$
$K^- p \rightarrow K^- p$	α

results which follow from the above are

$$\frac{d\sigma}{dt}(\bar{p}p \to \pi^+\pi^-) = \frac{\sigma_a(1-z^2)}{s^8}\left[\alpha(1-z)^{-2} + \beta(1+z)^{-2}\right]^2 \qquad \text{(VC.6)}$$

and

$$\frac{d\sigma}{dt}(\bar{p}p \to K^+K^-) = \frac{\sigma_a(1-z^2)}{s^8}\left[\alpha(1-z)^{-2}\right]^2 \qquad \text{(VC.7)}$$

which yields the ratio

$$\frac{d\sigma}{dt}(K^-p \to K^-p)/\frac{d\sigma}{dt}(\bar{p}p \to K^+K^-) = 2(1-z)^{-1} \qquad \text{(VC.8)}$$

The above results have been confirmed by the recent calculation of Matveev et al. (1974) who assume α=2, β=1, and γ_5 invariance (at high energies).

In the case of nucleon-nucleon scattering, the general treatment of the angular distribution taking into account the spins of the four external baryons and the six internal quarks is extremely complicated. The proton wavefunction was treated in leading order as a quark bound to a spin-one core, and spin effects were then treated exactly in the work of Blankenbecler, Brodsky and Gunion (1973). It was found that the dominant invariant amplitudes were the vector and axial-vector ones and hence that s-channel helicity was conserved in this limit. In the paper by Matveev et al. (1973) dimensional counting behavior of s^{-10} and s-channel helicity conservation were assumed. They then obtained an angular distribution that was somewhat different from Blankenbecler, Brodsky and Gunion near 90^o and quite different for smaller angles. An important point here is that the lack of antiquarks in the nucleon wavefunction means that the (st) graph does not occur in leading order and the (ut) graph (with final particle symmetrization) dominates the interchange amplitude.

All of these types of models predict that the dependence on energy and angle factor into the form

$$\frac{d\sigma}{dt}(pp \to pp) \sim s^{-n} R(z) + O(s^{-n-1}) \qquad \text{(VC.9)}$$

A check of this separation is shown in Fig. IVB.1 and Fig. IIA.8. The best fit value of n depends somewhat on the kinematic range involved. The angular dependence following from these models is also quite restricted and can be characterized by

$$R(z) = (1-z^2)^{-6} J(z) \qquad \text{(VC.10)}$$

where J(z) is slowly varying. This is again in reasonable agreement with the data. A precise calculation of J(z) is very model dependent and very difficult.

A severe test of any model is to take the matrix elements and to use them in both the direct and crossed channels. It is very instructive to first consider models where a single vector meson exchange dominates the amplitude. The magnitudes of the angular distribution of pp and $\bar{p}p$ elastic scattering in this case are comparable around 90^{o}, except for identical particle effects. If there are only neutral vector mesons then np should also be similar to $\bar{p}p$ in the backward hemisphere and have no backward peak. The data seems to rule out this scattering mechanism on both counts. Experimentally, the angular distribution of $\bar{p}p$ is strongly suppressed relative to pp and $np \to np$ has a backward peak.

In contrast the differential cross section that one gets in the CIM by crossing from Eq. (VC.10) can be characterized by the form

$$\frac{d\sigma}{dt}(\bar{p}p \to \bar{p}p) = s^{-n}(1-z)^{-6} \bar{J}(z) \qquad \text{(VC.11)}$$

where $\bar{J}(z)$ is slowly varying. The value of $\bar{J}(0)/J(0)$ is also predicted, and we shall return to this point in the next section. Also, the CIM amplitude for $np \to np$ is found to peak in the backward hemisphere.

One of the difficult questions to answer in interchange models concerns the prediction of the absolute normalization of the scattering amplitude. A detailed model of the hadronic wavefunction is required as well as a careful calculation of all the contributing diagrams. The most careful treatment for proton-proton scattering seems to be the work of Hayashi and Yabuki (1974). They assumed the quark-core model of the nucleon and find for the scattering amplitude in the spinless case

$$\frac{d\sigma}{dt} \cong \pi^3 (2m_V)^{16}\, m^{-4}\, s_0^4 (1-z^2)^{-6}\, s^{-12}\, \ell n^2 (s/s_0) \qquad \text{(VC. 12)}$$

where m is the effective parton mass and the nucleon form factor has the behavior

$$F(q^2) \cong (m_V/q)^4\, \ell n\, (q^2/s_0) \qquad \text{(VC. 13)}$$

so that $m_V^2 \cong 0.71\ (\text{GeV}/c)^2$. The value of m required to fit the data is very small and lies in the range 30-50 MeV if $s_0 = 1\ (\text{GeV})^2$. An important question is whether or not the inclusion of spin and the effects of the large numbers of coherent exchanges that contribute to the process modifies this result substantially.

Finally, it should be remarked that the energy dependence at fixed angle for resonance production is the same as for elastic scattering in this model. For example, the fixed angle cross section for $pp \to N^*p$ or N^*N^* should fall in energy at the same rate as pp elastic, and similarly for $\pi p \to \pi N^*$, ρN or ρN^*. The angular dependence for these latter processes should be different in general, and a measurement of their characteristic shape would help determine the properties of relevant wavefunctions.

LIST OF FIGURES FOR SECTION VC

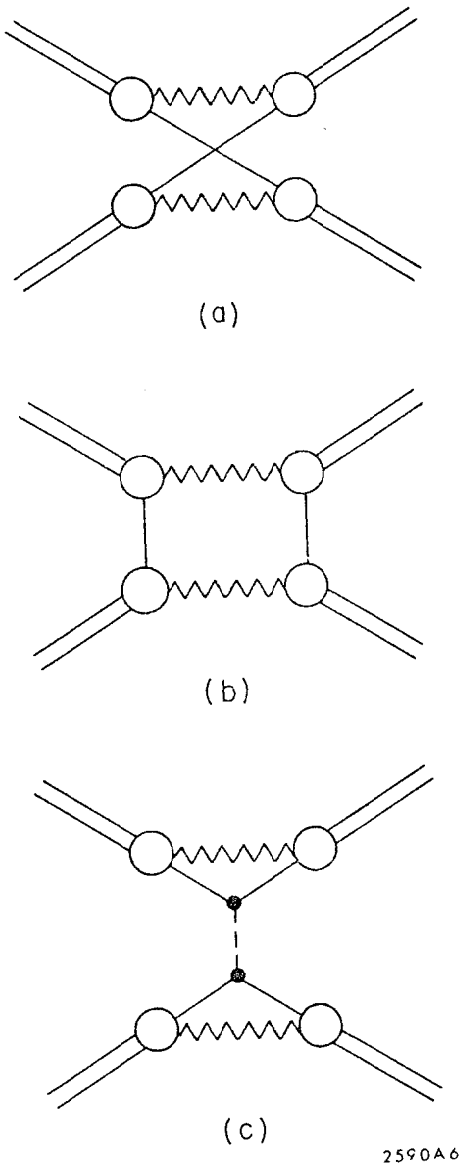

FIG. VC.1

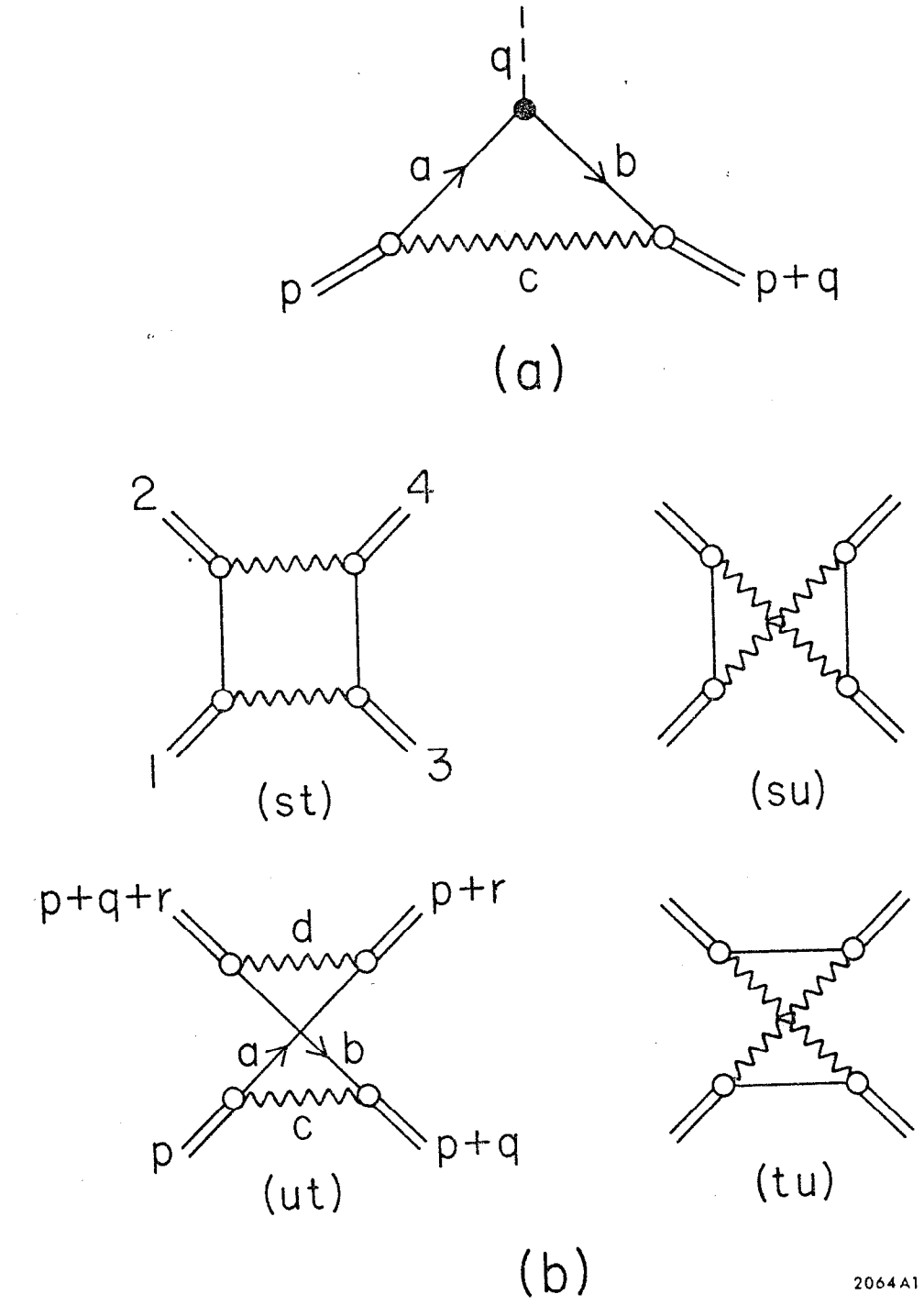

FIG. VC.2

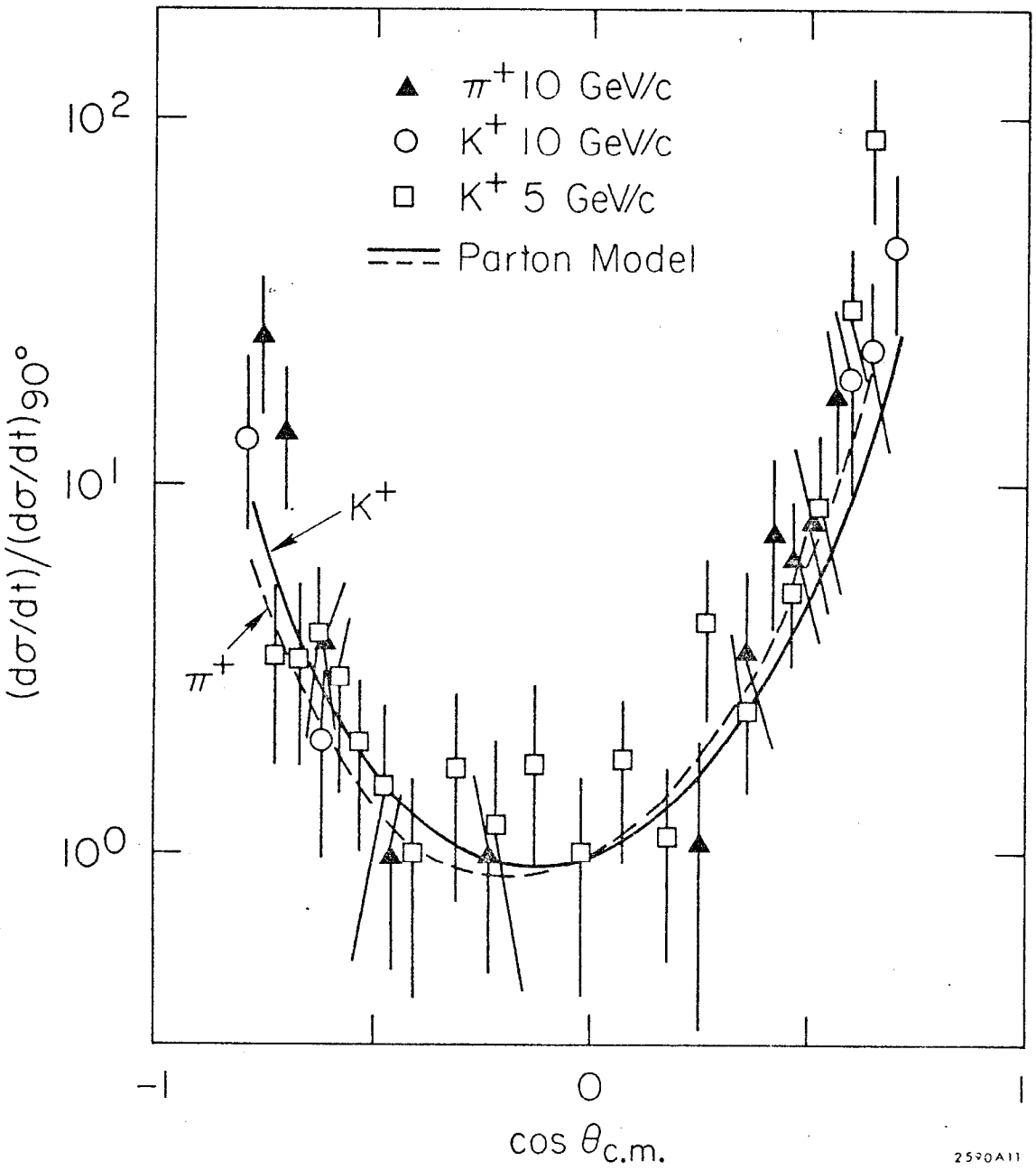
π^+ 10 GeV/c
K^+ 10 GeV/c
K^+ 5 GeV/c
Parton Model
10^2
10^1
10^0
$(d\sigma/dt)/(d\sigma/dt)_{90°}$
K^+
π^+
−1
0
1
cos $\theta_{c.m.}$
2590A11

FIG. VC.3

D. Fixed-Angle and Regge Behavior in the CIM

We have seen that the typical basic scattering process between hadrons falls with energy at fixed angle rather rapidly in the CIM. This is true even at fixed momentum transfer unless there is a direct vector gluon force (which we have argued must be negligible). The basic scattering process can be considered as in Fig. VD. 1a. If it falls as s increases at fixed t, then the system will prefer to scatter through diagrams of the form shown in Fig. VD. 1b. In this virtual bremsstrahlung diagram, particle A converts to H with a fraction x of the incident momentum and other coherent "stuff" with momentum (1-x). The basic process is thereby converted to $H+B \to H'+D$ scattering at the reduced effective energy $s' \approx xs$. If x can be small, then this process is not suppressed much if H' can pick up the momentum fraction (1-x) and convert to C. This latter process is suppressed as t increases, so that in the large t and eventual fixed angle limit, the irreducible process (Fig. VD. 1a) will dominate. At small t, the short circuit diagram will dominate and the cross section will fall less rapidly in s. This is the typical origin of Regge behavior in this model at small t. It is dominated by the emission and absorption of the less massive hadronic states. They therefore control the long distance or small-t behavior of the amplitudes.

As discussed earlier, the amplitude for the process $A+B \to C+D$ can be separated into the form

$$M \sim \beta_{BD}(t)\ (-u)^{\alpha_{ac}(t)} + \beta_{BD}(t)\ (-s)^{\alpha_{AC}(t)} + \ldots \qquad \text{(VD. 1)}$$

for fixed t as $s \to \infty$. The asymptotic behavior of the trajectory α_{AC} at large $|t|$ is controlled by the basic process which in this case (see Fig. VC. 1a) is quark-hadron scattering. It can be shown that the dominant diagrams using

quark counting lead to

$$\alpha_{AC}(-\infty) = \frac{1}{2}\,(4 - n_A - n_C - n_I) \qquad \text{(VD. 2)}$$

$$\beta_{BD}(t) \sim \tilde{\beta}_{BD}(t) \sim (-t)^{1/2(n_I - n_B - n_D)} \qquad \text{(VD. 3)}$$

where n_I is the minimum number of exchanged quarks.

These predictions do not automatically lead to factorization of residues as is required of t-channel singularities in Regge theory. For example, the above formula predicts that $\alpha_{\pi p}(-\infty) = -1$ and $\alpha_{pp}(-\infty) = -2$, but, of course, factorizable poles must contribute to both processes. In this case, the coupled channel T-matrix equations automatically force a cancellation between asymptotically degenerate trajectories so that the above relations are satisfied (Blankenbecler, Brodsky, Savit and Gunion, 1973). It was shown that the coupled (in the t-channel) system of meson-meson and baryon-antibaryon scattering has an amplitude of the form (neglect signature)

$$M = \beta^+(t)\,(-u)^{\alpha_+(t)} + \beta^-(t)\,(-u)^{\alpha_-(t)} + \beta_0(t)(-u)^{\alpha_0(t)} + \ldots \qquad \text{(VD. 4)}$$

where in the particular case studied,

$$\begin{aligned} \alpha_+(t) &\sim -1 + O(-t)^{-2} \\ \alpha_-(t) &\sim -1 + O(-t)^{-4} \\ \alpha_0(t) &\sim -2 + O(-t)^{-2} \end{aligned} \qquad \text{(VD. 5)}$$

and the β's depend on the channel involved. For meson-meson scattering, $\beta^+ \sim (-t)^{-1}$ and $\beta^- \sim -(-t)^{-4}$. Hence the fixed angle behavior is given by the first term. For meson-baryon scattering, $\beta^+ \sim (-t)^{-2}$ and $\beta^- \sim (-t)^{-2}$, and the fixed angle behavior arises from the first two terms. Finally, in the baryon-baryon case, $\beta^+ = -\beta^- \sim (-t)^{-3}$, and the first two terms tend to cancel with a remainder

of the order of $(-u)^{-1}\,(-t)^{-5}\,\ell n(-u) \propto s^{-6}\,\ell n\, s$ at fixed angle. The third term then dominates at fixed angle since it is of order $(-u)^{-2}\,(-t)^{-2} \propto s^{-4}$ at fixed angle.

It should be noted that the cancellation between the two leading trajectories in baryon-baryon scattering should occur when $\alpha^+ \cong -1$, since α^- is expected to be quite flat. Now α^+ is the trajectory that dominates pion-nucleon scattering and the effective trajectory extracted from the data seems to reach (-1) for $|t| \gtrsim 2\text{-}3\ \text{GeV}^2$. Thus one should expect the fixed angle power behavior s^{-10} for t's larger than this value and the behavior for smaller $|t|$ values depends in detail on the behavior of $\beta_+(t)$.

In some models, the leading trajectories for pp and πp scattering both approach the same value, but there are still degenerate trajectories at that value in order to produce the correct residues. In other models, the trajectories continue to fall logarithmically, see Baker and Coon (1971).

A detailed fit to $\bar{p}p \to \pi^-\pi^+$ and K^-K^+ at low energies has been carried out by Donnachie and Thomas (1974) who add the CIM term to a conventional Regge expansion with granddaughter trajectories. The CIM is important at low energies and low momentum transfer in their fit, perhaps because of the weakness of baryon exchange. Their form of the amplitude can be interpreted in terms of Eq. (VD.5), since the first term contains the ordinary Regge meson resonances on $\alpha_+(t)$ and its recurrancies. The second term is essentially a fixed pole since $\alpha_-(t) \cong -1$ for all reasonable $|t|$ and $\beta^- \cong (-t)^{-2}$—which is exactly in the CIM form.

The counting rules determine the asymptotic behavior of exotic as well as nonexotic trajectories. For example, $\alpha_{pp}(-\infty) = -2$ whereas the exotic double baryon exchange trajectory $\alpha_{pp}^{-}(-\infty) = -4$ and the corresponding residue is constant. Since the forces in exotic channels should be much weaker than in

nonexotic ones, one might expect that $\alpha_{\bar{p}p}(u)$ remains near $\alpha_{\bar{p}p}(-\infty)$ for all u whereas the residue need not remain constant for small u. If this is the case, then $\frac{d\sigma}{dt}(\bar{p}p)$ will vary as $s^{2\alpha-2} \sim s^{-10}$ throughout the backward hemisphere; this is consistent with the present data even in the backward (exotic) peak.

It should be noted that the predicted matrix elements for a given signature are of the form $\beta(t)\left[(-u)^{\alpha} \pm (-s)^{\alpha}\right]$. This form is to be used to extract the effective trajectory from the data even at large t, where $|u|$ is not $\cong s$ as is required in the usual Regge formula. The effective trajectories extracted from pp and $\pi^- p$ elastic data are shown in Fig. IIIA.4. It is the trajectory extracted in this manner which is to be compared with the CIM predictions. This was discussed in some detail in Section IIIA.

LIST OF FIGURES FOR SECTION VD

VD.1 (a) The irreducible contribution to hadron-hadron scattering. By definition H_0 (virtual) hadronic bremsstrahlung occurs before the interaction of A and B.

(b) Virtual hadronic bremsstrahlung contribution leading to Regge behavior of the scattering amplitude.

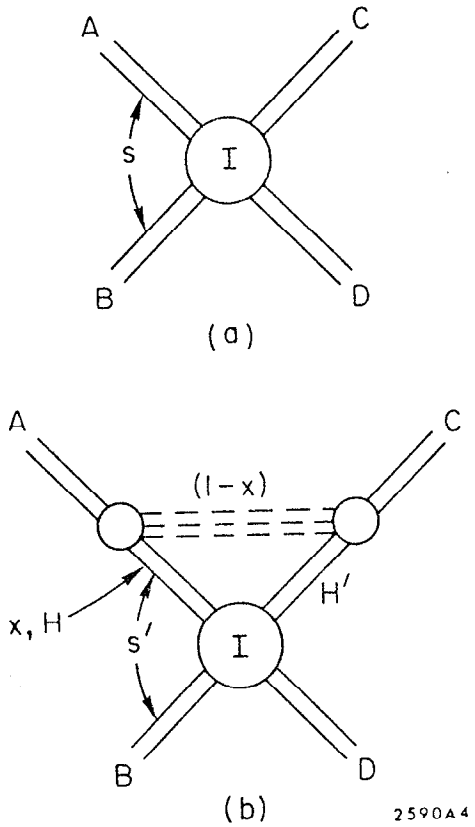

FIG. VD.1

E. Decay Distributions

The functions $G_{H/A}(x)$ have been introduced to describe the fractional longitudinal momentum distribution in a Lorentz frame in which $p_A \to \infty$ (see Appendix B). It is possible in fact to determine important features of G(x) by making measurements using other experimental observables which allows one to correlate decay properties of heavy systems, such as the timelike photon in e^+e^- decay with photoproduction, for example. Other examples which may be interesting to study are $\bar{N}N$ annihilation and the decay of heavy diffractively produced states.

The function $G_{H/A}(x)$ describes the breakup of A into the off-shell state H and a remainder. The decay of an unstable state A will reflect the threshold behavior of G in a new experimental context. In terms of the usual center-of-mass variable $\omega = 2E_H/M_A$, the inclusive decay $A \to H+X$ is described by

$$\frac{d\Gamma}{d\omega} \equiv d_{H/A}(\omega) \qquad \text{(VE. 1)}$$

In terms of a variable which is more like an infinite momentum frame variable, namely $x \equiv \left(E_H+p_H^z\right)/M_A$, where z is an arbitrarily chosen direction, the decay distribution is

$$\frac{d\Gamma}{dx} \equiv D_{H/A}(x) = \int_0^1 d\omega \left(\omega^2-4M_H^2/M_A^2\right)^{-1/2} d_{H/A}(\omega)\, \theta\left[\omega-x-M_H^2/xM_A^2\right] . \qquad \text{(VE. 2)}$$

The distribution vanishes if x is too near 0 and 1 and is naturally peaked at $x=M_H/M_A$.

Using the model described in Appendix A, the momentum distribution is given by

$$G_{H/A}(x) = \frac{x}{2(1-x)} \int d^2k_T\, db^2\, \rho(b^2)\, \phi^2(xS)\, [xS]^{-2} \quad , \qquad \text{(VE. 3)}$$

where $0 < x < 1$ and

$$S(k_T, x) \equiv M_A^2 - \frac{M_H^2 + k_T^2}{x} - \frac{b^2 + k_T^2}{1-x} \quad , \tag{VE.4}$$

where b^2 is the (mass)^2 of the "core" and $\rho(b^2)$ is its distribution. The decay distribution is easily computed by evaluating the imaginary part of the self-energy diagram. The decay width is easily seen to be

$$\Gamma \propto \mathrm{Im} \int \frac{dy}{1-y} d^2k_T \, db^2 \, \rho(b^2) \, \phi^2(yS) [yS]^{-2} \quad . \tag{VE.5}$$

If ϕ^2 is chosen to fall as a power of its argument, then it is easy to see that for x and ω near 1,

$$\begin{aligned} G_{H/A}(x) &\sim (1-x)^{g(H/A)} \\ d_{H/A}(\omega) &\sim (1-\omega)^{g(H/A)-1} \end{aligned} \tag{VE.6}$$

and hence

$$D_{H/A}(x) \sim (1-x)^{g(H/A)} \quad . \tag{VE.7}$$

The measurement of the decay functions $d_{H/A}(\omega)$ and $D_{H/A}(x)$ will provide independent evidence as to whether the dimensional counting rules are correct in general. An exciting possibility is to measure the threshold behavior in nuclear-nuclear collisions. The nucleons are the relevant constituents at low energies, and as the energy increases, the quark degrees of freedom should thaw and eventually become manifest. This transition would be very interesting to study—it could yield important information on the correct treatment of composite states.

F. Characterization of Inclusive Reactions

In this section a rough characterization of some selected inclusive cross sections in the central region will be given to illustrate the strong quantum number dependence of the predicted limiting behavior as $\epsilon \to 0$. The integral $I(x_1, x_2)$ defined in Eq. (VB.13) will be omitted in this discussion but should be included in any detailed numerical fit to the data over large ϵ range. In the previous sections we saw that the contribution of a particular basic process was described by the two numbers F and N. The value of F, the forbiddeness, measures the number of fields that must be radiated by the incident systems to arrive at the given basic process plus the number that must be radiated by c to produce the observed particle C. The value of N depends on the number of fields that are involved in the basic interaction process that produces the large angle scattering. It should be stressed at this point that the precise rules for which basic processes are allowed depend upon details of the quark confinement mechanism. Many choices are allowed within the CIM framework.

A comparison with the local effective powers F_{eff} and N_{eff} for data from ISR and FNAL as discussed by Blankenbecler, Brodsky and Gunion (1975) is also given in this section. Finally, the existence of quasi-elastic peaks in the data for particle-antiparticle differences will be discussed since it can provide an important confirmation of the overall hard scattering picture.

In order to clarify the formulae to follow, consider some typical basic CIM processes and the types of states that they contribute to (M = any meson state, B = any baryon state):

N = 4 (6 quarks involved)	N = 6 (8 quarks involved)
$M + q \to M + q$	$M + M \to M + M$
$\bar{q} + q \to M + M$	$q + (qq) \to M + B$

$q + q \rightarrow B + \bar{q}$ $\qquad$ $B + q \rightarrow B + q$

$\bar{q} + (qq) \rightarrow M + q$

$q + \bar{q} \rightarrow B + \bar{B}$

N = 8 (10 quarks involved)

$B + M \rightarrow B + M$

$B + (qq) \rightarrow B + (qq)$

$(qq) + (qq) \rightarrow B + q$

The case of N=2, quark-quark scattering, will not be considered further.

The inclusive cross sections will be written in the standard form

$$\frac{E d\sigma}{d^3 p}(AB \rightarrow C+X) = \left(p_T^2 + m_4^2\right)^{-4} Q_4(C, \epsilon) + \left(p_T^2 + m_6^2\right)^{-6} Q_6(C, \epsilon) + \ldots \quad \text{(VF.1)}$$

where the dependence of the Q function on the angle has been suppressed as has the dependence on the target, incident beam, and detected particle. Only the terms with the minimum values of F will be explicitly written. However, one should keep in mind that as the energy increases for fixed p_T, $\epsilon \rightarrow 1$, and larger F values can be expected since extra bremsstrahlung becomes more and more favored. Our discussion is not meant to be exhaustive but only to indicate the general features expected.

The most important terms in reactions of the type $pp \rightarrow CX$ where $C = \pi^{\pm,0}$, K^+, η, $\rho^{\pm,0}$, etc. are expected to involve N=4 and 6 from the above table. Higher values of N may be present of course, but they should be damped by the large p_T and finite ϵ values involved in present experiments. It is straightforward to count the minimum amount of bremsstrahlung necessary and one finds

$$Q_4(\pi, \epsilon) = h_1 \epsilon^9 + h_2 \epsilon^{11} + h_1' \epsilon^{13} + \ldots \quad \text{(VF.2)}$$

where the h_1' term can arise from the same processes that produce the h_1 term with the emission of an additional mesonic $(q\bar{q})$ pair. Also

$$Q_6(\pi, \epsilon) = h_3\epsilon^5 + \ldots \qquad \text{(VF.3)}$$

The "constants" h_i depend on the choice of C and depend on x_1, x_2 through the integral $I(x_1, x_2)$.

In the reaction $pp \rightarrow K^-X$, which might be termed "forbidden", the initial state has no quarks in common with those in K^- and more bremsstrahlung is required to connect them. One finds

$$Q_4(K^-, \epsilon) = h_2\epsilon^{11} + h_1\epsilon^{13} \qquad \text{(VF.4)}$$

and

$$Q_6(K^-, \epsilon) = h_3\epsilon^9 + \ldots \qquad \text{(VF.5)}$$

Note that if the ϵ^{11}process $(q+\bar{q} \rightarrow M+M)$ dominated both the K^- and K^+ reactions, then the ratio (K^-/K^+) would be constant. In general, however, one might expect that this ratio will fall as ϵ^2 or ϵ^4 as ϵ decreases.

The reaction $pp \rightarrow pX$ is an interesting one because it involves a more complex trigger particle which is also present in the initial state. It has several new types of subprocesses that contribute to it. The basic process $q+q \rightarrow B+\bar{q}$ will ultimately produce a p_T^{-8} behavior if it is present, but one might expect that those mechanisms that dominate the exclusive scattering amplitude should be very important (that is, $q+B \rightarrow q+B$ and $(qq)+B \rightarrow (qq)+B$). These involve a large N value but should be dominant at small ϵ. There is also the (possible) basic process $(qq) + (qq) \rightarrow B+q$ that is the only one that requires double fragmentation and also contributes to leading order in the inclusive limit (s^{-10}).

The cross section should be characterized by the forms

$$
\begin{aligned}
Q_4(p, \epsilon) &= H_1 \epsilon^7 + \ldots \\
Q_6(p, \epsilon) &= H_2 \epsilon^3 + H_3(M) \epsilon^5 + H_4(\bar{B}) \epsilon^{11} + \ldots \\
Q_8(p, \epsilon) &= H_5 \epsilon + H_6 \epsilon^3 + H_7(\bar{B}) \epsilon^{11} + \ldots \\
Q_{10}(p, \epsilon) &= H_8 \epsilon^3 + \ldots
\end{aligned}
\qquad \text{(VF.6)}
$$

The term $H_3(M)$ is written so as to emphasize that an associated meson system is produced with the proton and these terms should be comparable in the two cross sections. Similarly for $H_{4,7}(\bar{B})$, so that in the antiproton cross section should look like

$$
\begin{aligned}
Q_4 &\quad \text{small} \\
Q_6 &= \bar{H}_4(B) \epsilon^{11} + \ldots \\
Q_8 &= \bar{H}_7(B) \epsilon^{11} + \ldots
\end{aligned}
\qquad \text{(VF.7)}
$$

where consistency demands that $\bar{H}_4(B)$ and $\bar{H}_7(B)$ are of the same magnitude as $H_4(\bar{B})$ and $H_7(\bar{B})$ extracted from a fit to the proton data.

It is of particular importance in understanding the basic dynamics of large p_T reactions to compare experiments with different beam particles. This degree of freedom allows one to change the predicted F value for a given N value and to check the normalization of the basic subprocesses. One important process is clearly $\pi p \rightarrow \pi X$ which is expected to be of the form

$$
\begin{aligned}
Q_4(\pi, \epsilon) &= k_1 \epsilon^7 + k_2 \epsilon^5 + k_3 \epsilon^3 + \ldots \\
Q_6(\pi, \epsilon) &= k_4 \epsilon^3 + k_5 \epsilon + k_6(B) \epsilon^5 + \ldots
\end{aligned}
\qquad \text{(VF.8)}
$$

The k_3 and k_5 terms do not Feynman scale but they do contribute to the exclusive limit behavior of s^{-8}. They involve the basic processes $\pi+q \rightarrow \pi+q$ and $\bar{q}+p \rightarrow \pi+(qq)$ respectively. The $k_6(B)$ term produces a recoil baryon system and it should also show up in the reaction $\pi+p \rightarrow pX$. Other final states can be discussed in a similar manner.

The final process to be described here is the reaction $\bar{p}p \rightarrow \pi X$ that allows the possibilities of new types of basic processes. The cross section can be written in terms of

$$Q_4(\pi, \epsilon) = K_1\epsilon^9 + K_2\epsilon^7 + \ldots$$
$$Q_6(\pi, \epsilon) = K_3\epsilon^3 + K_4\epsilon^5 + K_5\epsilon + \ldots \qquad \text{(VF.9)}$$

where the K_3 term arises from the process $(qq)+(\bar{q}\bar{q}) \rightarrow \pi+M^*$, and K_4 from $\bar{q}+(qq) \rightarrow \pi+q$. The K_5 term is the only one that contributes to leading exclusive behavior of s^{-8} and involves $\bar{p}+(qq) \rightarrow \pi+\bar{q}$ and $p+(\bar{q}\bar{q}) \rightarrow \pi+q$. Without extra bremsstrahlung it does not Feynman scale. Detailed fits to data are necessary to determine which diagrams are important. Such fits can be found in Raitio and Ringland (1975).

The characterizations given above emphasize that there are two distinct limits involved here which are sometimes confused in the literature. They are (1) large p_T with ϵ (or x_T) fixed in which the minimum value of N eventually dominates, and (2) $\epsilon \rightarrow 0$ with p_T fixed in which the minimum value of F dominates. This should be kept in mind since it is often stated that <u>the</u> parton model (not further defined) predicts a factorization for $x_L \sim 0$:

$$\frac{E d\sigma}{d^3p} \simeq \left(p_T^2 + m^2\right)^{-N} f_N(\epsilon) \quad . \qquad \text{(VF.10)}$$

We see that this is correct if one sums over possible values of N in the above formula. This sum is absolutely necessary since, in general, different terms with different N values will dominate in the two limits defined above.

However, this form suggests two important and complementary ways of extracting information from data. Since $f_N(\epsilon)$ is predicted to behave as ϵ^F for sufficiently small ϵ, this provides the motivation to define effective powers $N_{eff}(\epsilon)$ and $F_{eff}(p_T)$ by the equations

$$N_{eff}(\epsilon) = -p_T^2 \frac{\partial}{\partial p_T^2} \ell n\left(\frac{Ed\sigma}{d^3p}\right) \qquad \text{(VF.11)}$$

where the derivative is taken at fixed ϵ and θ_{CM}, and

$$F_{eff}(p_T) = \epsilon \frac{\partial}{\partial \epsilon} \ell n\left(\frac{Ed\sigma}{d^3p}\right) \qquad \text{(VF.12)}$$

which is calculated at fixed p_T and θ_{CM}. These two functions can be extracted directly from the data. They provide not only an immediate first test of any theory, but also a guide in determining the types of terms involving different values of N and F that are required in a detailed fit and estimates of the masses required. The N and F values then provide clues as to what type of basic processes are important which then leads to the type of final state correlations that are to be expected. The functional dependence of N_{eff} and F_{eff} can be computed in models as per Eq. (VB.12). Because of the variation of the integral $I(x_1, x_2)$, F_{eff} can vary from F as G increases even if one term dominates.

The extractions for the BS data from the ISR and the CP data from FNAL a are shown in Figs. VF.1 and VF.2. Since mass corrections will affect the shape of N_{eff} at small p_T, decreasing its value there, and since N_{eff} must vanish at $p_T = 0$ if the process is to Feynman scale, the experimental results clearly show the presence of N=4, 6, and 8 terms as expected and show little difference between particle-antiparticle. The F_{eff} curves, however, can be quite different for various particle types. Their values clearly tend to increase as the energy increases although the errors on F_{eff} are quite large from the

ISR. The F_{eff} curves for K^- and $\bar{p}$ are higher than for the other particles, reflecting more bremsstrahlung, and are quite flat, reflecting an origin in the pionization region. The F_{eff} value for protons is quite small, especially in the FNAL range, characteristic of fragmentation and the protons presence in the initial beam. For the further details on the analysis of these curves, we refer the reader to the original paper (Blankenbecler, Brodsky and Gunion, 1975).

An interesting application of how the N_{eff}, F_{eff} analysis can be used to predict correlations is provided by the reaction $\mu p \to \pi X$. Here we expect two leading contributions, (a) $N=2$, $F=5$ corresponding to the usual parton subprocess $\mu + q \to \mu + q$ where the large p_T of the π is balanced by the muon, and (b) $N=3$, $F=4$ corresponding to $\gamma q \to \pi + q$ in which the recoil momentum is taken up by a jet of hadrons. Another important application of this analysis is the process $pp \to \mu X$, since it separates the Drell-Yan $N=2$ process from hadron-produced muons.

These F_{eff} curves also display an important feature of hard scattering models which provides an important check of the presence of a small number of constituents. This feature is the presence of quasi-elastic peaks in the x_T distribution corresponding to the most likely momentum distribution among the constituents involved in the basic subprocess. For this configuration the cross section will peak as a function of x_T and hence F_{eff} must vanish there. This is only seen in the difference between particle and antiparticle cross sections since then the Pomeron component (which peaks at $x_T = 0$) cancels, allowing the valence part of the wave function to be observed.

The inclusive cross section can be written as an integral over z, the cosine of the C.M. scattering angle in the subprocess (set $\tilde{G}_{C/c} = \delta(x_c - 1)$):

$$\frac{E d\sigma}{d^3 p} \propto \int_{-(1-2x_1)}^{(1-2x_2)} \frac{dz}{(1-z^2)} F_{a/A}\left(\frac{2x_1}{1+z}\right) F_{b/B}\left(\frac{2x_2}{1-z}\right) \frac{d\sigma}{dt}\left(s' = \frac{4p_T^2}{1-z^2}, z\right) , \quad \text{(VF.13)}$$

where $F(y) = yG(y)$. Now the valence part of the probability function should be peaked at the values of y corresponding to the zero binding limit. That is, the first one should be peaked at $x_a = n_a/n_A$, where $n_A = n_a + n(\bar{a}A)$, and n_a is the number of constituents in the state a. Similarly for $G_{b/B}$. If these peaks in the integrand control the values of z, that is, if the angular dependence of $\frac{d\sigma}{dt}$ is sufficiently mild, then there is a peak in the integral at the value

$$x_T = \hat{x}_T \equiv 2\left[\frac{n_A}{n_a} \operatorname{ctn} \frac{\theta}{2} + \frac{n_B}{n_b} \tan \frac{\theta}{2}\right]^{-1} , \quad \text{(VF.14)}$$

where θ is the C.M. scattering angle of C. Thus the scattering arising from the valence part of wavefunction should have an $F_{eff} = 0$ at this value of x_T (for example, at 90^o, and for $n_A/n_a = 3$, $n_B/n_b \cong 5$, $\hat{x}_T \cong 1/4$). If there is final state bremsstrahlung, the value of $\hat{x}_T$ should be multiplied by $n_C/(n_C + n(\bar{C}c))$.

The analysis for the differences $(K^+ - K^-)$ and $(p - \bar{p})$ are shown in Fig. VF.3. The difference between π^+ and π^- is of the same size as the errors, and this analysis cannot be made in this case. We see that F_{eff} does seem to vanish in both the ISR (at $\hat{x}_T \sim .1$) and FNAL (at $\hat{x}_T \sim .2$) energy ranges. The relative values are consistent with the fact that larger F_{eff} values are found at the higher energies. The absolute values are reasonable if important small x_T Regge terms are still present in the difference of cross section.

A final simple consistency check is to examine the exclusive limit of the processes analyzed above. The exclusive limit cross section should fall as a

power of s given by $N_{ex} = 1+N+F$. From the CP data, $(N_{ex})_{eff}$ is estimated to be ~ 12.5 for $\pi^{\pm}$ and K^{+}, ~ 14 for K^{-}, ~ 13 for p and ~ 17 for $\bar{p}$. The values are higher by 1 or 2 for the BS data. These results are to be compared with the minimum possible values, which are 12, 14, 10, and 16 respectively, but a given subprocess will in general have a larger N_{ex}. The particular values are in reasonable agreement with expectations and the relative ordering is as expected.

Photon Processes

Large transverse momentum processes involving photons are particularly important tests of the hard-scattering models and the counting rules (IVB.1-IVB.10) since they directly probe the point-like nature of the constituents. If the photon is counted as an elementary field, an explicit breakdown of vector dominance in the large momentum regime is predicted. The measurement of $\gamma p \to \pi p$ at fixed angle by Anderson et al. (1973) at SLAC gives $d\sigma/dt \sim s^{-7.3\pm0.4}$ and is consistent with the dimensional counting prediction of s^{-7}, although higher energy tests are required. Predictions for the angular distribution are given by Scott (1973). A gauge invariant parton model for photoproduction is given by Mueller-Kirsten and Hite (1974). We emphasize that Compton scattering at large t will provide a decisive test of the electromagnetic structure of hadrons. Parton model (see Brodsky, Close and Gunion, 1972; and Landshoff and Polkinghorne, 1972) and light-cone analyses (see Frishman, 1972) demand the existence of a J=0 fixed pole contribution to the Compton amplitude. Thus, for sufficiently large |t| (where normal trajectories recede to negative values)

$$\frac{d\sigma}{dt}(\gamma p \to \gamma p) \propto \frac{1}{s^2} F^2(t) \quad , \qquad s \gg |t| \tag{VF.15}$$

with $F(t) \propto t^{-2}$, consistent with s^{-6} dimensional counting fixed angle prediction. Measurements of interference effects in $e^{\pm}p \to e^{\pm}p\gamma$ can test the prediction that

the fixed pole contribution is independent of photon mass at fixed t. These and other related tests are discussed by Brodsky, Close and Gunion (1973).

Deep inelastic Compton scattering $\gamma p \to \gamma X$ and pion photoproduction $\gamma p \to \pi X$ at large p_T are very interesting and basic inclusive tests for any parton model. The asymptotic cross section $Ed\sigma/d^3p\,(\gamma p \to \gamma X)$ is predicted to be scale-invariant and proportional to the sum of quark charges to the fourth power (Bjorken and Paschos, 1969). However present experiments are kinematically restricted in the small-t domain and thus can be expected to be sensitive to non-leading contributions in p_T. The conventional and expected contributions to $\gamma p \to \gamma X$ and $\gamma p \to \pi^o X$ arising from (a) $\gamma + q \to \pi + q$ and $\gamma + q \to \gamma + q$ subprocesses are illustrated in Fig. VF.4, with additional, nonleading terms arising from the subprocesses $\bar{q} + B \to \pi + (qq)$ and $\bar{q} + B \to \gamma + (qq)$. Just as in the hadronic case, the latter type of diagrams—which have a minimum number of spectator quarks—are expected to be especially important at small ϵ. It is perhaps easiest to think of these as arising from the baryon scattering off of the $(\bar{q}q)$ components of the target photon. Using the counting rules as given before, the expected cross sections are

$$\frac{Ed\sigma}{d^3p}(\gamma p \to \pi X) = \frac{J_1\epsilon^3}{\left(p_T^2+m^2\right)^3} + \frac{J_2\epsilon^0}{\left(p_T^2+m^2\right)^6} + \ldots \qquad \text{(VF.16)}$$

and

$$\frac{Ed\sigma}{d^3p}(\gamma p \to \gamma X) = \frac{J_1'\epsilon^3}{\left(p_T^2+m^2\right)^2} + \frac{J_2'\epsilon^0}{\left(p_T^2+m^2\right)^5} + \ldots \qquad \text{(VF.17)}$$

The ϵ^0 terms (which also include the usual electromagnetic logarithmic factor) would be ϵ^1 if the photon were pure vector meson dominated so that it would act like a $q\bar{q}$ state rather than a fundamental field.

The photoproduction process has been analyzed by Eisner et al. (1974) at $p_{LAB} = 21$ GeV/c for π^o and they find $N_{eff} \cong 6-7$ and $F_{eff} \cong 0.5$ with $m^2 \cong 0.5-1.2$ GeV^2. Boyarski et al. (1974) have analyzed $\pi^{\pm}$, $K^{\pm}$, and $p^{\pm}$ data at 18 GeV/c and for the charged pion case find a reasonable fit with $N_{eff} \cong 6$ and $F_{eff} \cong 1$. In the case of deep inelastic Compton scattering, the SLAC measurements of the Santa Barbara group (Eisner et al., 1974) give a fit with $N_{eff} \cong 4.5$, $F_{eff} \cong 0.5$, and $m^2 \cong 0.8$ GeV^2. Further the ratio of $\gamma p \to \gamma X$ to $\gamma p \to \pi^o X$ does seem to be consistent with the predicted $p_T^2 + m^2$ behavior; despite the extra factor of α. The cross sections should eventually become of comparable magnitude. Note that if $\gamma p \to \gamma X$ is measured at large t, away from the edge of phase space, we still expect the scale-invariant parton model prediction to hold at large p_T. Finally, we also mention that the difference of cross sections for $e^{\pm} p \to e^{\pm} \gamma X$ at large photon mass and large p_T measures the interference of Bethe-Heitler and virtual Compton amplitudes and the sum of the cube of the parton charge (see Brodsky, Gunion, and Jaffe, 1973). Because of the interference nature of this measurement, background terms of the J_2' type cannot contribute. A light-cone analysis of this process is given by Kiskis (1974).

LIST OF FIGURES FOR SECTION VF

VF.1 Plots of N_{eff} and F_{eff} from the ISR-CCR data for the reaction $pp \rightarrow \pi^{o}X$ for three energy pairs. The statistical errors are of the same size as the discrepancies from different energy pairs.

VF.2 Plots of N_{eff} and F_{eff} from the ISR-BS and FNAL-CP data for charged particles. The FNAL energy pairs are (19.4 - 23.8 GeV) marked by x's and (23.8 - 27.4 GeV) marked by dots.

VF.3 F_{eff} for particle-antiparticle differences illustrating the peak in ϵ as F_{eff} vanishes.

VF.4 The basic processes discussed in the text for inclusive (a) photoproduction and (b) Compton scattering.

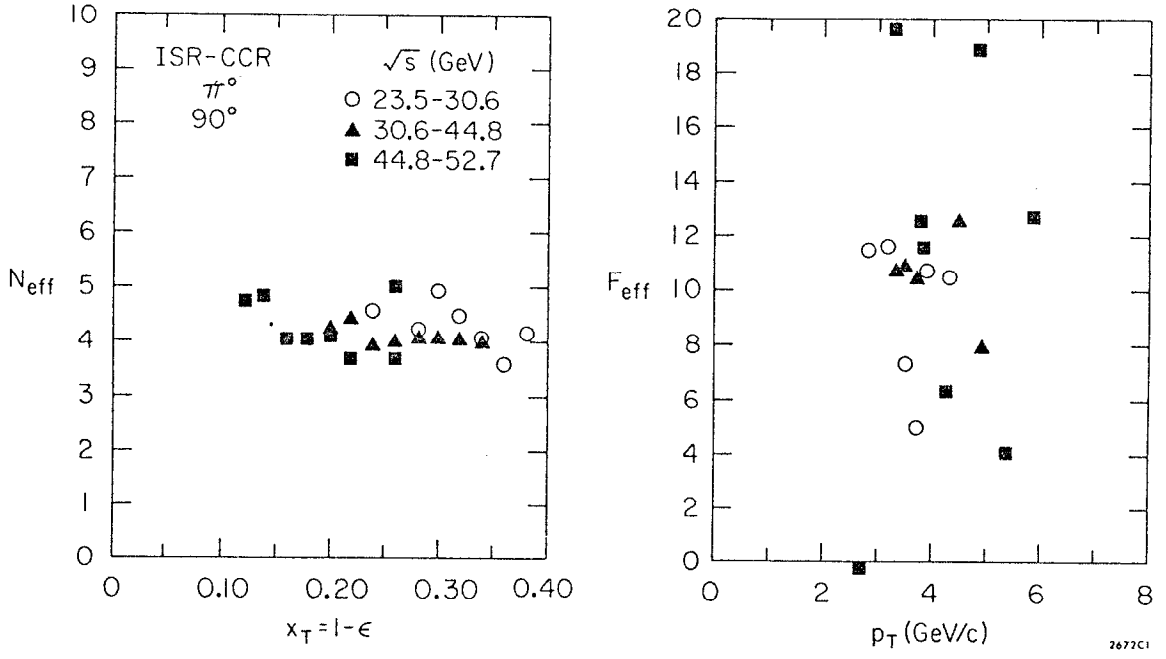
ISR-CCR
π°
90°
√s (GeV)
23.5-30.6
30.6-44.8
44.8-52.7
N_eff
x_T = 1 - ϵ
F_eff
p_T (GeV/c)
2672C1

FIG. VF.1

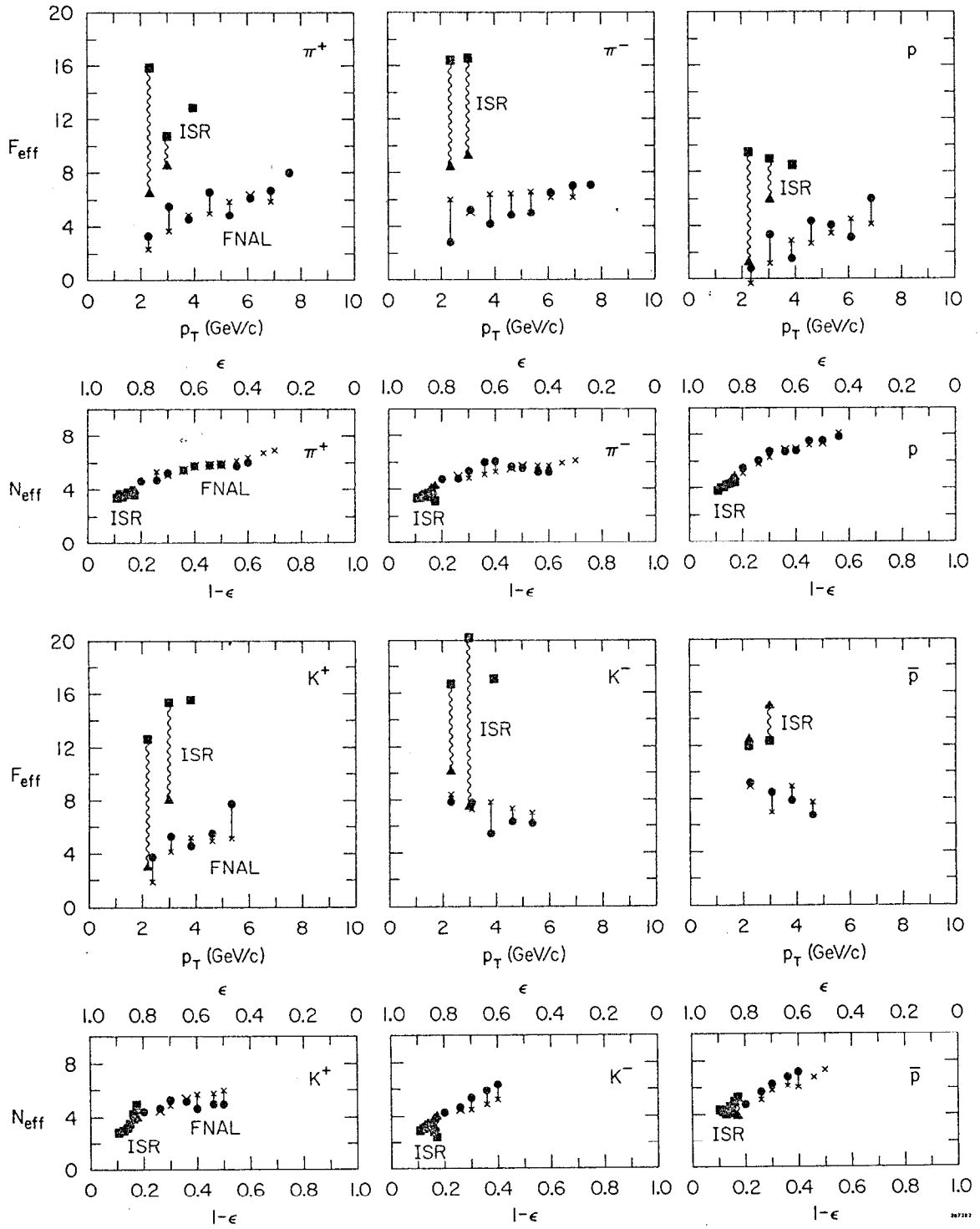

FIG. VF.2

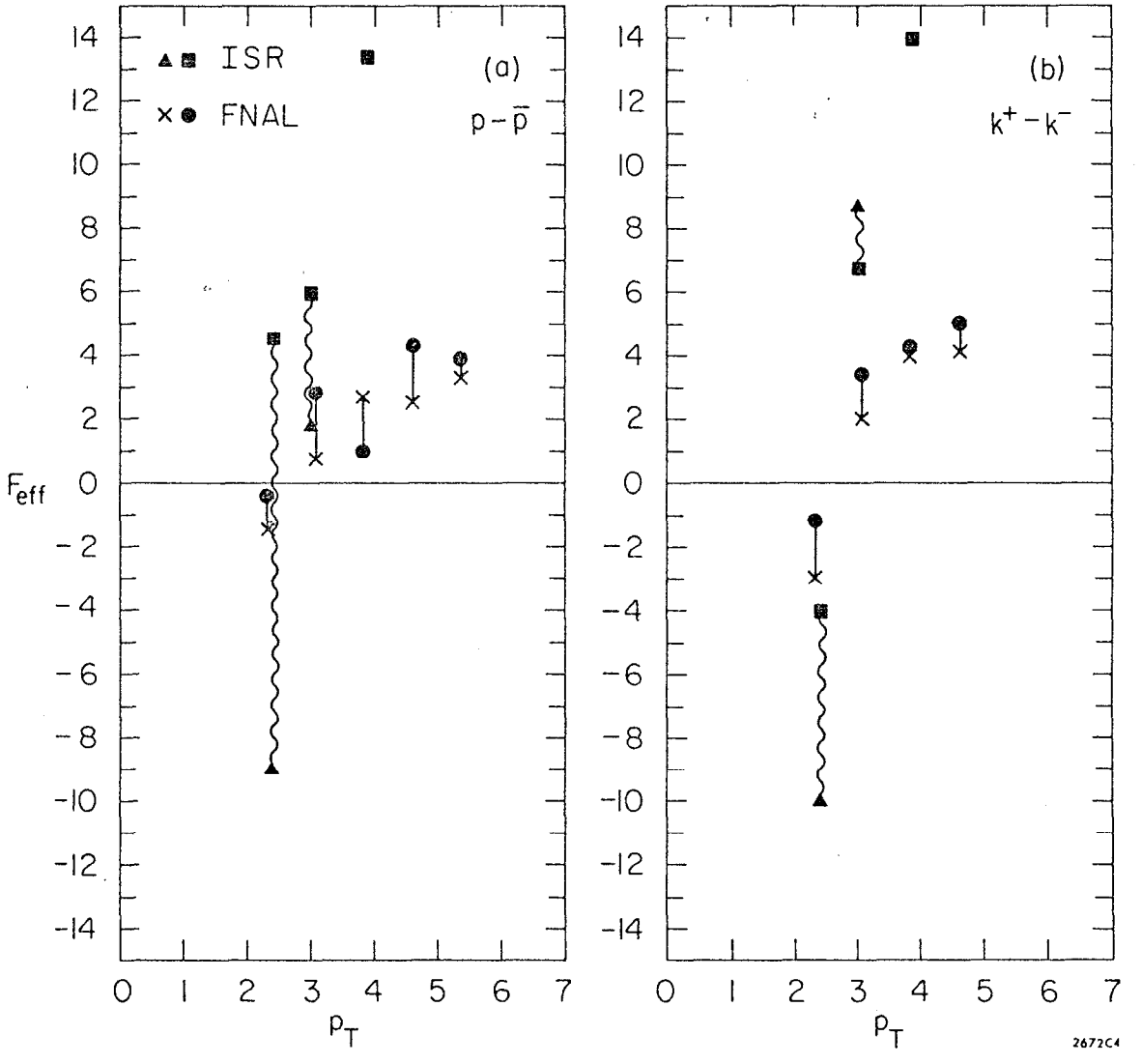

FIG. VF.3

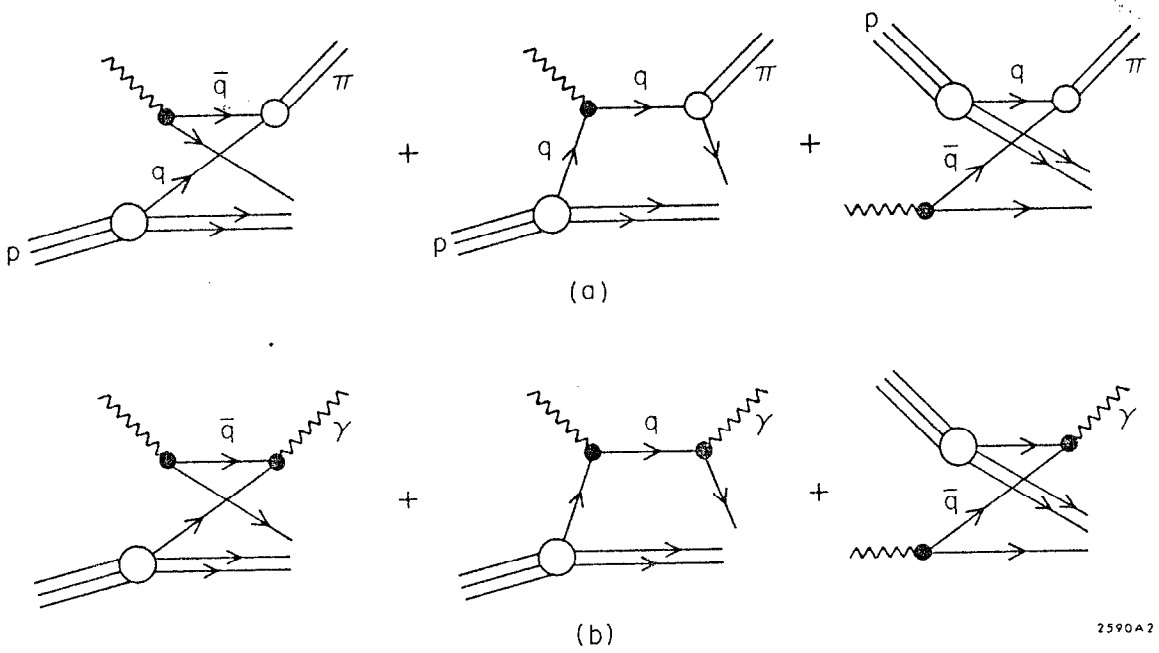

FIG. VF.4

G. Theoretical Expectations for Correlations Involving Large p_T Hadrons

Thus far, there has not yet been a great deal of theoretical work on inclusive correlations involving a large p_T hadron in spite of the fact that this area should provide fertile ground for new theoretical insights. The simple theoretical work which has been done suggests that correlations are crucial in disentangling the underlying dynamic mechanisms. The preliminary data on correlations have provided hints of unexpected phenomena. The opportunities for further progress here are many.

One aspect of the problem of correlations which has apparently caused some misunderstanding involves p_T conservation. It is important to recall that the way in which transverse momentum is conserved depends on the underlying dynamical mechanism so that it is not possible to isolate momentum conservation as a separate kinematic effect. The following simple example will illustrate this point. Assume that the absolute square of the matrix element for an event with n+1 particles can be written in the form

$$|M(p_1 \ldots p_{n+1})|^2 \propto f(p_{T1}) \ldots f(p_{T(n+1)}) \qquad \text{(VG. 1)}$$

This is just the assumption of the "uncorrelated jet model" (Krzywicki, 1964) or transverse cutoff phase space which is often used as an example of a model without dynamical correlations. If we then trigger on an event containing a large p_T particle, we have the constraint

$$-\vec{p}_{T(n+1)} = \vec{p}_T = \sum_{i=1}^{n} \vec{p}_{Ti} \qquad \text{(VG. 2)}$$

If we neglect energy conservation this is the only source of correlations in transverse momentum in the model. We can see, however, that the implications of the constraint depend on the form of the $f(p_{Ti})$. If, for example, the f's are

gaussian

$$f(p_{Ti}) \propto e^{-bp_{Ti}^2} , \qquad \text{(VG. 3)}$$

the preferred way to satisfy (VG. 2) is for each of the n particles to be clustered around the point p_T/n. In contrast, if $f(p_T)$ has a simple power falloff the preferred configuration is where one recoil particle has a large p_T and the others are near the origin. We may therefore find something like the phase space configuration found in hard collision models without assuming any underlying 2-2 hard process.

The fundamental test of an underlying 2-2 mechanism is, of course, the coplanarity of events containing large transverse momentum particles. As discussed in IIC, this follows from the assumption that the constituents and the products of hadronic bremsstrahlung have limited transverse momentum relative to the beam direction so that the probability functions, $G_{a/A}(x,\vec{p}_T)$, Eq. (A.8), in hard collision models are sharply peaked at small p_T. Gunion (1974) has suggested that it is consistent with the spirit of hard collision models that the probability functions themselves have slow power-law-behavior in their high p_T tails so that the implied convolutions over p_T can give significantly larger deviations from coplanarity than might otherwise be expected. It has not yet been demonstrated, however, that the broad azimuthal correlations observed by the CCR group can be obtained in this manner. Also, it detracts from the conceptual simplicity of hard scattering models when all the mechanisms leading to large p_T are not explicitly isolated. One possibility is that significant contributions from inclusive generalizations of multiple-scattering diagrams are necessary to achieve the experimentally observed noncoplanarity of large p_T events. The azimuthal correlations give an indication that while the hard scattering models

may be able to explain data on large p_T production, there remains a substantial gap in our understanding.

An alternate way to approach the jet hypothesis which temporarily avoids confrontation with the fact that there be significant noncoplanarity in the events is to look for evidence of the underlying hard collision in the quantum number structure of an event. The basic idea is that the quantum numbers of the particles with large p_T should, in some statistical sense, be related to the quantum numbers of the constituents participating in the hard collision. For example, if we give up the idea of a scale-invariant quark-quark cross section but assume that quark-quark scattering is the dominant internal mechanism, we would predict that the large p_T hadrons should reflect the quantum numbers of the valence quarks of the incident beams. For pp collisions, the observed surplus of positive over negative particles at large p_T is in crude agreement with this idea.

At the level of two particle correlations, the quark-quark scattering mechanism does not lead to significant correlations between the quantum numbers of one large p_T jet and those of the jet on the opposite side. There are only the overall constraints due to charge-conservation, etc. In contrast, the constituent interchange model contains many possible internal hard-scattering mechanisms. Yet, if the model is correct,by triggering on a large p_T particle with definite quantum numbers, experiments can select the particular mechanisms that dominate. This mechanism must be consistent with the observed single particle spectrum. An example discussed by Newmeyer and Sivers (1974) consists of triggering an apparatus on a large p_T proton and looking in the opposite hemisphere for p's or $\bar{p}$'s. If quark-scattering is the dominant mechanism, the opposite hemisphere jet should contain the usual surplus of baryons over

antibaryons expected in the fragmentation region of a quark. In the CIM, however, triggering on a large p_T baryon may select a substantial contribution from the hard subprocess $qq \rightarrow B\bar{q}$. Here an antiquark is balancing the large p_T of the baryon and we expect a surplus of antibaryons over baryons in the opposite hemisphere jet. Simple model calculations for

$$R = \frac{<p> - <\bar{p}>}{<p> + <\bar{p}>} \qquad \text{(VG.4)}$$

where $<p>$ is the average number of protons and $<\bar{p}>$ the average number of antiprotons in the hemisphere opposite a large p_T proton are shown in Fig. VG.1 as a function of the x_T of the trigger particle. At FNAL energies, the subprocess $q+qq \rightarrow M+B$ may be important, predicting the dominance of mesons opposite a triggered baryon.

Another example of the importance of quantum number constraints involves the production of strange particles in the CIM. The tendency is for strangeness to be balanced between opposite large p_T jets. In pp collisions of a large p_T meson where the leading irreducible mechanism is $qM \rightarrow qM$, the strangeness transfer components

$$u\pi^o \rightarrow sK^+$$
$$d\pi^+ \rightarrow sK^+ \qquad \text{(VG.5)}$$
$$\text{etc.}$$

lead to jets containing opposite strangeness. The process $uK^+ \rightarrow uK^+$, however, balances the strangeness of a jet with a particle in the fragmentation region.

Another important question is whether correlations involving large p_T hadrons are related to the clustering properties of low p_T events. In models such as the CIM the participating hadrons in the subprocess can be resonances. Since energy-momentum constraints would imply a negative correlation between

two particles with large transverse momentum in the same direction if all hadrons were produced singly, the observation of positive same side correlations is already sufficient to guarantee that there is some clustering. It remains open whether it is intrinsically different from the clustering observed among low p_T particles. For a review of cluster models, see Ranft (1974).

As emphasized by Bjorken (1974) there are several relations between the invariant cross sections for clusters and the invariant cross section for their decay products in the limit where angle or rapidity is approximately conserved by the "soft" decay process. Let us assume that the invariant cross section for the production of a cluster,

$$\frac{Ed^3\sigma^c}{d^3p}(\vec{p}, s) \cong \frac{1}{p_T^n} f^c(p/p_{max}, \theta_{CM}) \qquad \text{(VG.6)}$$

approximately exhibits power law scaling and assume a scaling law (see VE.2)

$$\frac{dN_c}{dx} = D_{h/c}(x) \qquad \text{(VG.7)}$$

for the decay of the cluster into hadrons, where

$$x \cong |\vec{p}_h| / |\vec{p}_c| \cong p_T^h/p_T^c \qquad \text{(VG.8)}$$

since the angles are approximately the same. We then have

$$\frac{Ed^3\sigma^h}{d^3p}(\vec{p}, s) \cong \frac{1}{p_T^n} \int_z^1 dx\, x^{n-2} f^c\left(\frac{z}{x}, \theta_{CM}\right) D_{h/c}(x) \qquad \text{(VG.9)}$$

where $z = p_T^h/p_T^{max}$. Because the effective power of n in (VG.6) is usually quite large it is the behavior of $D_{h/c}(x)$ near x=1 which determines the form of the

power law scaling for the decay products

$$f^h(z, \theta_{CM}) \cong \int_z^1 dx\, x^{n-2} f^c\left(\frac{z}{x}, \theta_{CM}\right) D_{h/c}(x) \ . \qquad \text{(VG. 10)}$$

In interpreting the correlation function

$$R = \sigma_{inel} \frac{E_1 E_2 d\sigma/d^3p_1 d^3p_2}{\left(E_1 d\sigma/d^3p_1\right)\left(E_2 d\sigma/d^3p_2\right)} - 1 \qquad \text{(VG. 11)}$$

for two large p_T hadrons in approximately the same direction we see that a large amount of the p_T dependence is due to the variation of the single particle distributions. If we assume that both particles come from a cluster with momentum $\vec{p} = \vec{p}_1 + \vec{p}_2$ and $\mathcal{M}^2 = (p_1 + p_2)^2$ and then normalize that invariant cross section to the invariant cross section for a single hadron at momentum $\vec{p}$

$$\frac{\dfrac{E d\sigma}{d^3p\, d\mathcal{M}^2\, dx\, d\phi}}{\left(\dfrac{E d\sigma}{d^3p}\right)_n} \cong \frac{R\left(E_1 d\sigma/d^3\vec{p}_1\right)\left(E_2 d\sigma/d^3\vec{p}_2\right)}{2\sigma_{inel}\left(E\, d\sigma/d^3\vec{p}\right)}$$

with $x = E_1/E$. As pointed out by J. Bjorken, if the cross section for producing a high p_T system reflects strongly the total p_T and is not a rapidly varying function of the internal variables, this should be a slowly varying function of p_T. An estimate of the function based on CCR data on $\pi^o\pi^o$ correlations is shown in Fig. VG. 2 as a function of p_T. The fact that it is reasonably constant supports the general assumptions.

The interpretation of correlations in specific models has only now begun. Uematsu (1974) has shown that the energy dependence of two particle distributions in the model of Berger and Branson (1973) is quite large. Formulas for two-particle correlations in the quark scattering model are given by Ellis and Kislinger (1974), and these can be readily generalized to other hard scattering models.

The correlation in θ_{CM}, or the rapidity variable $\eta = \log \tan (\theta_{CM}/2)$ between opposite side particles reflects both the angular dependence of the active subprocess and the distribution of momentum in $G_{a/A}(x)$, $G_{b/B}(x)$, $G_{C/c}(x)$, and $G_{D/d}(x)$. A subprocess with an isotropic distribution is already ruled out by the data, since it produces much too narrow an angular correlation, compared to the $\Delta\eta \sim 3.5$ correlation width measured by the Pisa-Stony Brook group at $\sqrt{s} = 52$ GeV with one particle at $\theta_{CM} = 90^{o}$ and $p_T > 3$ GeV. Angular dependences such as $d\sigma/dt \sim t^{-4}$ or u^{-4} which might be expected in modified gluon exchange models, or the forms $d\sigma/dt \sim 1/su^3$, u/s^5, $1/s^2u^2$, which are possible for $q+\pi \rightarrow q+\pi$ are not inconsistent with the Pisa-Stony Brook data measured at $x_T \sim 0.1$ since the data in this region are sensitive to the small-x behavior of the structure functions. However, at larger x_T, the predicted differences between the various models for $d\sigma/dt$ are very distinct. Calculations valid at large x_T have been given by Ellis (1974b). Multiparticle correlations also should be able to discriminate between these models.

Recent experiments have also determined the correlation in η as a function of the CM angle of the detected large p_T particle. If two different distributions $G_{a/A}(x)$ and $G_{b/B}(x)$ occur, as in $\pi+q$, then the C.M. tends to be "thrown" in the direction of the "heavier" of the particles a and b. In the case of an isotropic $d\sigma/dt$, one expects events to have an "antiback-to-back" correlation, i.e., the particles on the opposite side of the detected high p_T particle should have the same sign of p_L^{CM}. However, if $d\sigma/dt(a+b \rightarrow c+d)$ is forward or backward peaked, then the above effect can be negated, and a back-to-back correlation can occur. Future measurements of these correlations, especially at higher momentum transfers and with complete momentum determination will be very useful

discriminants of the models. Generally, the features of the correlations are expected to sharpen as p_T increases. More extensive computations of the angular distributions and fits to the inclusive spectra are being carried out by Raitio and Ringland (1975).

LIST OF FIGURES FOR SECTION VG

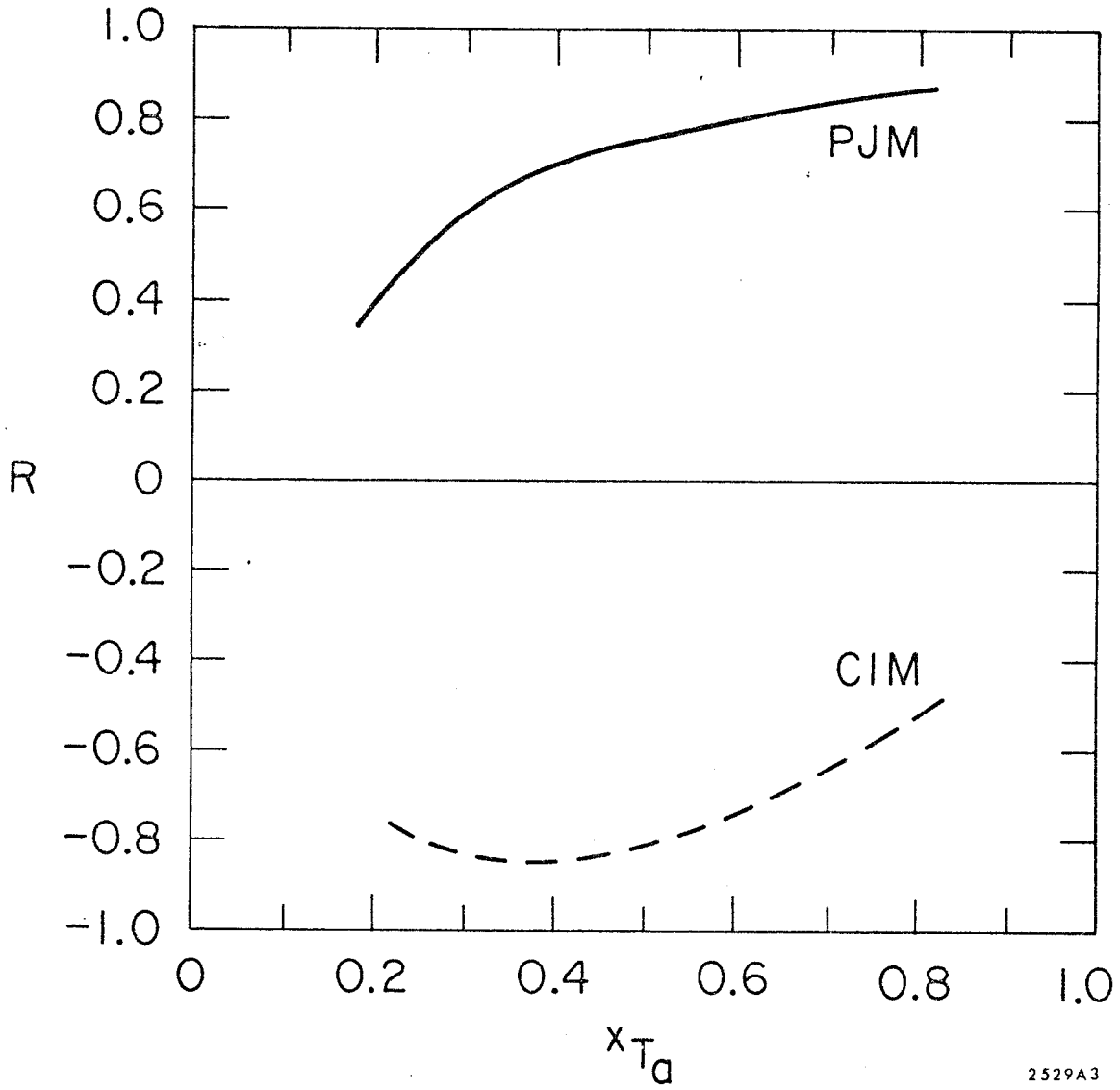

FIG. VG.1

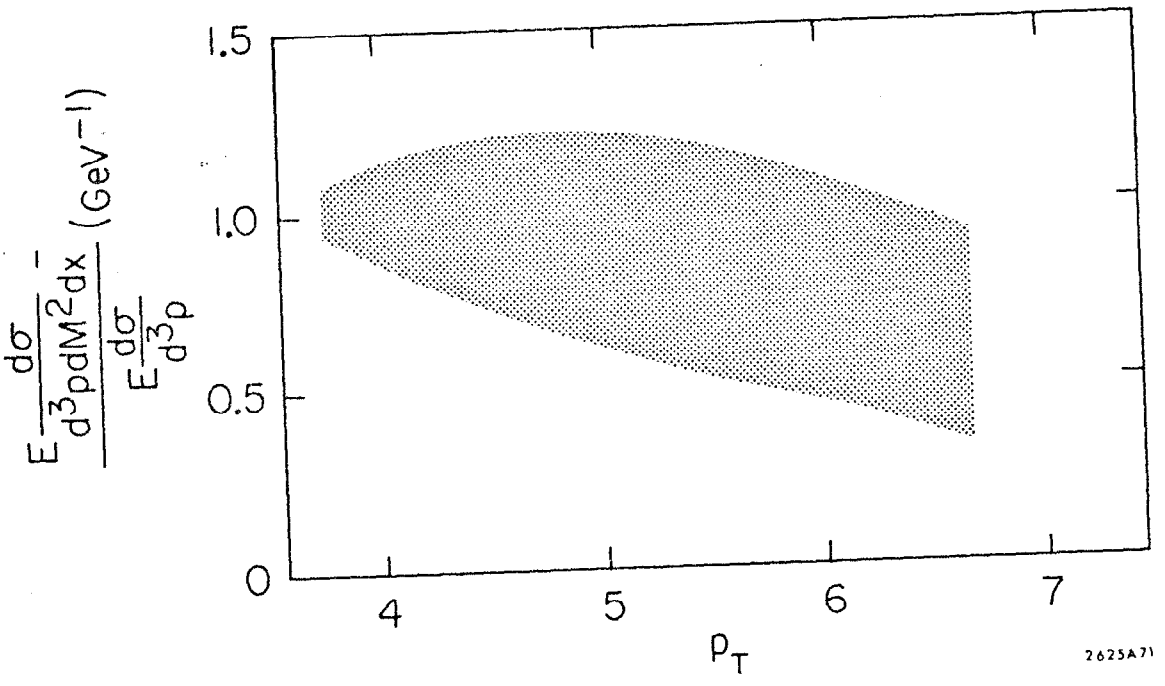
$E\frac{d\sigma}{d^3pdM^2dx}$ (GeV^{-1})
$E\frac{d\sigma}{d^3p}$
1.5
1.0
0.5
0
4
5
6
7
p_T
2625A71

FIG. VG.2

H. The Production of New Particles and Large p_T

A very intriguing question arises concerning whether a large fraction of the observed high-transverse-momentum hadrons could be related to the production of new particles. Lederman (1975) has advanced the speculation that essentially all the hadrons produced in excess of an $\exp\left(-6p_T\right)$ extrapolation are the decay products of heavy particles related to the $\psi(3100)$ and $\psi(3700)$ observed at SPEAR (Augustin et al., 1974) and at BNL (Aubert et al., 1974).

In support of this view one can note that the SPEAR data suggest the existence of a threshold at $\sqrt{s}$ = 3-4 GeV resulting in the approximate doubling of the ratio $\sigma(e^+e^- \rightarrow \text{hadrons})/\sigma(e^+e^- \rightarrow \mu^+\mu^-)$. This could be translated into an effective threshold for the production of hadrons at large p_T in pp collisions. Except perhaps for the associated multiplicities of the Argo Spectrometer group (A. Ramanauskas et al., 1973) there is as yet no evidence for this type of threshold structure but it may emerge in careful analysis of new data. Further support of the idea can be found in the fact that

$$\frac{d\sigma}{dt}(\gamma p \rightarrow \psi p) \propto e^{at} \quad , \qquad a \cong 2\frac{1}{2} - 3 \tag{VH. 1}$$

(Knapp et al., 1975). This corresponds to the general picture of the growing importance of heavy particles at large t and is consistent with the idea that the ψ's are more pointlike than ordinary hadrons.

As discussed in Section III, the most important constraint on this suggestion is the observed small and constant value of the ratio

$$\mu/\pi \cong 10^{-4} \tag{VH. 2}$$

in pp collisions. If the leptonic/nonleptonic decay ratios of the majority of these new particles is the same as observed for the ψ's

$$\frac{\Gamma(\psi \to \mu^+\mu^-)}{\Gamma(\psi \to \text{hadrons})} \cong 0.1 \qquad \text{(VII. 3)}$$

then very few of the large p_T hadrons can be their decay products.

It may be that the hard subprocess in the constituent pictures we have been discussing can be effectively replaced by a sum over high-mass low-spin resonances in the direct- and crossed-channel. This new type of duality could have many implications and could perhaps lead to a connection between events with a few high p_T hadrons and those with a large multiplicity of low p_T hadrons.

It should be noted that the production of ψ's in pp collisions is suppressed in heavy quark models by the operation of "Zweig's rule" which forbids a produced quark to end up in the same hadron as its antiquark. Thus the associated production of particles which carry the new quarks bound to the usual quarks should be favored. However, in those events in which there is a ψ, arguments can be made (Sivers, 1975b) which indicate that there should also usually be a pair of heavy hadrons. Moreover there should be local balancing in rapidity of the number of new heavy quarks so that the momentum of a high p_T ψ should be balanced by a recoil system containing the new hadrons.

Even if there is no direct connection between the existence of the new particle and the unexpected yield of high p_T hadrons, it is possible that large p_T physics can illuminate some of the properties of the ψ's. For example, a possible test of whether the ψ is an elementary spin-one particle or a composite $q\bar{q}$ system involves the comparison of fixed-angle scaling laws for $\gamma p \to \gamma p$ and $\gamma p \to \psi p$ or inclusive scaling laws for $\gamma p \to \gamma$ + anything and $\gamma p \to \gamma$ + anything. Note that the

observation of a J=0 fixed pole in ψ photoproduction,

$$\frac{d\sigma}{dt}(\gamma p \to \psi p) \propto s^{-2} f(t) \qquad \text{(VH.4)}$$

would be dramatic proof of the elementarity of the new state since Brodsky, Close and Gunion (1973) have shown that fixed-pole behavior is impossible in the photoproduction of composite systems. Whether or not these kinds of tests on the nature of the ψ are feasible, in view of the small observed cross sections, is difficult to say—the simple examples discussed here involve extremely small effects.

The production of heavy mass particles can, in principle, give us the same type of dynamical information sought in large p_T processes. An important mechanism for the production of heavy hadrons should be $q\bar{q} \to H\bar{H}$ so that the dynamics of the process may not be too different from $q\bar{q} \to K^-K^+$. This may be reflected in the scaling laws for the production processes. The production of heavy particles at large transverse momentum offers an opportunity to study how the parameter m^2, in the formula

$$\frac{Ed^3\sigma}{d^3p} \sim \frac{f(\epsilon)}{\left(p_T^2+m^2\right)^N} \qquad \text{(VH.5)}$$

depends on the internal masses (quark masses or hadron masses) in the problem. The production of new quantum numbers implies the existence, on the average, of a greater number of spectators, so the production of heavy hadrons should be dominated by the small x_T kinematic region. Photon, lepton and meson beams offer the best opportunity for isolating the presence of the new particles because of the improved signal-to-noise ratio due to the presence of antiquarks with large x.

It is possible to dimensionally analyze the production of heavy mass systems in much the same way as in large p_T inclusive reactions. Counting rules in the CIM for lepton pair production have been derived by Sachrajda and Blankenbecler (1975) which predict the behavior in mass ($\mathcal{M}$) and threshold ($1-\mathcal{M}^2/s$) for any incident beam and choice of basic process. These include both annihilation (Drell-Yan) and bremsstrahlung type contributions. The inclusive-exclusive connection was also discussed. It will be very helpful to have data of sufficient quality and quantity so that an effective power analysis can be performed. This would help distinguish between the possible basic processes that can contribute.

The presence of heavy narrow resonances offers the possibility of many interesting effects in inclusive channels. It is important to note the possibility that the anomalous energy behavior for large-angle $\bar{p}p$ elastic scattering between p_{LAB} of 5 and 6 GeV/c (T. Buran et al., 1974) may be due to the effect of the $\psi(3700)$ at the upper energy, $\sqrt{s} = 3.68$. The possibility that the "Ericson fluctuations" observed by Schmidt et al. (1973) may really be due to a new heavy baryon coupled weakly to $\pi^{\pm}p$ is also worth considering.

The discovery of the ψ and ψ' are important in that they demonstrated both the limitations and the virtues of current theoretical approaches to hadronic phenomena. For example, we now can only expect $R = \sigma(e^+e^- \rightarrow \text{hadrons})/\sigma(e^+e^- \rightarrow \mu^+\mu^-)$ to become asymptotic at some energy regime considerably above the masses of the new particles. Efforts to explain why this ratio did not agree with simple quark model predictions in the lower energy regime did not prove too illuminating. We must keep in mind that the simple quark model rules for large p_T processes discussed here may also fail in such a way as to unmask this new dynamics. If this "thawing" is due to the opening up of new degrees of freedom, they can be included in the counting rules in an obvious manner. If not, then we will be learning about a new type of hadronic matter.

VI. SUMMARY AND CONCLUSIONS

The detailed study of the properties of large-transverse-momentum phenomena is now just beginning and much more experimental and theoretical work will be required before definitive conclusions are possible. It does seem appropriate, however, to make the following preliminary observations.

The kinematic regime in which large p_T data is being collected is characterized by an invariant single particle inclusive cross section which displays a falloff somewhere between $\exp(-6p_T)$ and $(p_T)^{-4}$. These two predictions may be considered extremes, the first possibly valid at low p_T and the other possibly valid at some ultra-high p_T. We do not completely understand from the quark parton picture why there is no evidence for a $(p_T)^{-4}$ component in the present kinematic regime although there are speculations, based on models for quark binding, why such a term may be absent or suppressed. See Section IV.

The available data on single particle inclusives are observed to be smooth over a wide range of p_T and $\sqrt{s}$. There appears to be no sharp boundary between low p_T and high p_T regimes or between high energy and low energy dynamical mechanisms. However, we cannot be completely satisfied with this observation due to the presence of large gaps in the coverage of the high p_T, intermediate energy range. Data from SLAC, BNL, CERN-PS and Serpukhov are needed to test for this smoothness with greater precision. Data at these energies and $x_T \sim 1$ can also explore directly the connection between inclusive and exclusive cross sections.

The jet hypothesis, i.e., the assumption of an underlying hard scattering mechanism, can most easily be tested by looking at the complete phase-space structure of individual events containing a large p_T trigger. This type of data can give basic information on the internal dynamics. For example, there is speculation

that the inclusive "jet cross section"

$$E_{jet} \frac{d\sigma}{d^3(p_{jet})} \sim \frac{f(x_{jet})}{\left(p_{jet}^T\right)^4}$$

may display scale invariance, where $\vec{p}_{jet} = \Sigma_i p_i$ is the sum of the momenta of all particles in a given event with $p_{Ti} \gtrsim \langle p_T \rangle$. This cross section can be measured directly, e.g., in hadronic calorimeter experiments, and the speculation should be tested. The measurements of associated multiplicities and correlations at the ISR support the idea of some sort of broad jet structure. The results of the ARGO spectrometer measurements at BNL displaying a sharp rise in the associated multiplicity as a function of p_T constitute, at this time, the sole exception to the rule that physical observables extrapolate smoothly between small p_T and large p_T.

Hard scattering models are consistent with a large body of data. However, the observed lack of coplanarity in the two particle inclusive data provides an important challenge to this point of view. More data on azimuthal correlations, with different particles and in different kinematic ranges, is obviously in order. It is particularly interesting to check whether the coplanarity distribution changes at higher values of x_T. Comparisons with correlations observed from lepton and photon induced reactions will also be significant. It is also an interesting theoretical problem to see whether hard scattering models can be generalized in some way to avoid the prediction of coplanarity. This would be, in some sense, a retreat for this model but it could be balanced against other successes. The inclusion of "hard" 2-3 internal processes might be an interesting exercise.

For completeness we also mention other important experimental constraints. Measurements of the angular dependence of inclusive reactions are of obvious

importance in separating the dependence of cross sections on the distribution functions $G_{a/A}(x)$ and $G_{b/B}(x)$ and the angular dependence of the basic subprocesses. Correlation measurements between two or more large transverse momentum particles and their angular dependence will further constrain the form of the internal scattering cross sections. The distribution of momentum in the recoil system in principle can distinguish between subprocesses involving the production of jets, or systems of fixed mass.

Beams of γ's, π's, K's and $\bar{p}$'s are interesting from the quark model framework because they provide more antiquarks with a large fraction of the incident momentum. In general photon and meson beams have a larger fraction of their momentum available for high x_T processes compared to baryons. So far all large p_T experiments have been done with incident protons, but changing beams can have a dramatic effect on the large p_T cross sections for particles involving antiquarks. Photon experiments are valuable because γ's couple with approximately equal strength to all varieties of constituents and can provide a close connection with electroproduction data. The J=0 fixed pole in Compton scattering furnishes a real test for the pointlike coupling of the photon to some internal constituent. Unified planning of experiments with these new beams is necessary to provide related measurements over a wide kinematic regime.

The flow of quantum numbers in an event containing a large p_T particle provides a good discriminant for different models of the internal dynamics. The quark models provide a general constraints on the quantum numbers of the irreducible hard scattering process and specific models have definite predictions. Measurements involving the differences between different beam particles, detected particles, and n or p targets are sensitive to the valence and Regge components of the distribution functions. The most critical measurements of

quantum flow involve quantum number correlations. For example, in the CIM model for production in pp collisions, the detection of a K^- at sufficiently large x_T signals the presence of a K^+ in the opposite hemisphere. However, for different internal processes strangeness of a large p_T K^+ can be balanced by a K^-, by Λ's or Σ's in the fragmentation region or by Λ's and Σ's in the opposite jet. The study of correlations with particle identification in experiments involving a variety of beams and targets is obviously an important experimental goal. The use of quantum number flow to identify the important internal subprocesses can serve as an important consistency check on the identification of the subprocesses by "effective power" analysis.

The effective powers discussed in Section VF can provide an important phenomenological tool. They are quantities which can summarize concisely the systematic trends of the data and which can be extracted simply from models. In combination with the quark model and constituent counting they provide important clues to the important internal mechanisms. Analysis of data from FNAL and ISR results in plateaus in N_{eff} and F_{eff} at values consistent with expectations in the CIM. Particles and antiparticles are found to have similar N_{eff}'s but, as expected, display quite different F_{eff}'s. The correlation of N_{eff} and F_{eff} with the quantum numbers of the detected particles supports the general features of the quark model. The observation of peaks in $\epsilon = \mathcal{M}^2/s$ for the difference between particle and antiparticle cross sections provides supplementary evidence for the existence of a small number of internal constituents, each with a finite fraction of the hadron's momentum. Application of this type of analysis to new data over a wide range of energies, different angles and smaller ϵ values can help probe more deeply into the basic dynamics. We also emphasize that applications of the effective power analysis can greatly clarify the physics of the deep inelastic electromagnetic processes.

The use of nuclear targets in high p_T experiments has uncovered an interesting unexplained feature incidental to the original objectives of the experiments. The dependence of the data for meson production on the nuclear target type is found to vary as $A^{1.1}$ for $p_T > 3$ GeV/c. This is distinct from both the coherent $A^{2/3}$ and the incoherent A^1 dependence expected. The explanation of this fact is uncertain although there are many theoretical suggestions. More experiments on nuclear targets at different values of p_T and $\sqrt{s}$ are obviously appropriate. The structure of the recoil system for high p_T production on various nuclear targets can clarify the role of double scattering contributions.

The expectations for fireball models as a general description of large p_T processes has not been fully exploited. If parton models run into serious snags the idea that fireball approaches can be, in some sense, supplementary to hard scattering approaches might provide new insight into the problems.

In view of the evidence from SPEAR of scaling violations associated with the production of ψ's and/or heavy charmed particles, the possibility of a connection between large p_T production and heavy particle production should be explored fully. There may be an enriched sample of new heavy particles in events in which there is a large p_T hadron. Certain of the large p_T particles (e.g. direct muons) may come from the decay of new types of particles. From a more general view, the dynamics underlying the production of massive particles may be related in structure and form to the dynamics of large p_T. Constituent models provide a framework where this type of possible connection can be easily visualized (see Section VH).

In the area of exclusive experiments, improved high p_T data can probe several features of the strong interactions. An important test for the finite compositeness of hadrons is to check whether Regge trajectories asymptote to negative integers

or continue to fall at large $|t|$. The present data is not sufficient to decide this point. It is also important to test for fixed angle scaling, $d\sigma/dt \sim s^{-N} f(\theta)$, in $2 \to 2$ processes with more data. Measurements of the ratios of the differential cross sections $\gamma B \to \gamma B$: $\gamma B \to \pi B$: $\pi B \to \pi B$: $BB \to BB$ for a fixed range of $\theta_{C.M.}$ would provide an important check on the relative complexity of photons, mesons, and baryons. Present data agree with simple constituent counting laws but also display many features (zero structure, polarization, etc.) which are most easily understood in geometric terms. Data do not, however, display the shrinkage ($\sigma \sim \sigma(\Delta p_T \, \Delta b)$) implied by the asymptotic validity of geometric constraints. It is therefore an important question whether the geometrical features survive at higher energies. The search for Ericson fluctuations is also crucial in deciding the important question of the existence of heavy resonances.

It is also important to check the scaling laws for multiparticle exclusive processes for fixed invariant ratios such as $ep \to ep\pi$, $e^+e^- \to n\pi$, $p\bar{p} \to n\pi$, etc., and predictions for fixed angle cross sections related by crossing: $p\bar{p} \to p\bar{p}$: $pp \to pp$, $p\bar{p} \to \pi\bar{\pi}$: $\pi p \to \pi p$, etc. Another intriguing question is whether nuclear form factors and distribution functions can be predicted from constituent counting rules.

Most models that have been discussed in the text have been formulated to attempt to understand isolated features of large p_T events. It is usually very difficult to make other predictions in these models without which their overall validity cannot be tested. In contrast, the CIM models provides a unified framework to discuss exclusive reactions and inclusive processes over the entire Peyrou plot. The model is exceedingly simple in all these cases. It is consistent with the ideas tested in deep inelastic lepton scattering and hence provides a bridge between photo and hadronic processes.

At small momentum transfers, the model converts smoothly to the usual Regge--purely hadronic description of exclusive and inclusive reactions. In a sense the CIM gives a simple prescription for mapping duality diagrams to dynamics at short distances.

The predictions of the CIM can be discussed at two levels. The first level involves the general form of the cross sections and their dependence on specific kinematic variables. Thus, the exclusive differential cross sections are predicted to factorize at large angles in the form $g(s)\,f(\theta)$, and the form of Regge trajectories and residue functions are prescribed. At a more detailed level, the model predicts the specific functions involved for any process, and in the exclusive scattering case, $g(s) \sim s^{-N}$, where N is fixed by quark counting, and the function $f(\theta)$ is specified. Similar statements hold in the inclusive case.

Within the CIM framework, one must still specify the particular composite nature of the hadrons. For example, the nucleon can be considered to be a bound state of three equivalent quarks or of a quark and a core. These alternatives give different predictions in general for nucleon-nucleon scattering ($N = 10$ or 12 respectively). All of the constituent counting rules given in the text for inclusive scattering are based on the former model of the nucleon but the latter can be easily discussed. Experimental information is needed to decide between these possibilities.

Even though alternative models can do as well in describing some features of the data, the fact that there appear to be no violations of CIM predictions for form factors and exclusive or inclusive scattering is significant.

In spite of the empirical success of the CIM at large p_T and parton model ideas in deep electromagnetic scattering, there are important conceptual obstacles associated with the fact that quarks are assumed to be permanently bound. This

must affect the treatment of strong interactions at some level, but just where and how this will occur depends on the unknown binding mechanism. It is probably necessary to understand this binding before the final state configurations in inclusive reactions can be computed. Theoretical attempts in this direction have only scratched the surface.

Acknowledgments

We wish to thank J. Alonso, J. Bjorken, G. Farrar, R. Pearson, G. Ringland, R. Ristio, and D. Wright for many helpful conversations. We are particularly indebted to J. Gunion for his unlimited assistance.

APPENDIX A

DERIVATION OF THE HARD SCATTERING MODEL

All of the predictions of the various hard-scattering and parton models for large-transverse-momentum inclusive processes depend on the validity of an underlying probabilistic formula. In this appendix we derive the central equation for hadronic processes in a form sufficiently general to allow for transverse momentum fluctuations. Hard scattering model for the reaction $AB \to CX$ are based on a decomposition of the form indicated in Fig. I.5 where the final state, X, consists of contributions of particles and clusters from $p(A\bar{a})$, $p(B\bar{b})$, $p(\bar{C}c)$ and p(d). We write

$$d\sigma(AB \to CX) = \frac{1}{2E_A 2E_B \mid V_A - V_B \mid} \mid M_{AB \to CX} \mid^2 dp \qquad (A.1)$$

with the assumed decomposition

$$\mid M_{AB \to CX} \mid^2 = \sum_{ab,\,cd} \frac{\phi_A^2(p_a^2)}{(p_a^2 - m_a^2)^2} \frac{\phi_B^2(p_b^2)}{(p_b^2 - m_b^2)^2} \frac{\phi_C^2(p_c^2)}{(p_c^2 - m_c^2)^2} \mid M_{ab \to cd} \mid^2 \qquad (A.2)$$

and

$$dp = \frac{d^4p_C}{(2\pi)^3} \delta^{(+)}\left(p_C^2 - m_C^2\right) \frac{d^4p_{A\bar{a}}}{(2\pi)^3} \delta^{(+)}\left(p_{A\bar{a}}^2 - m_{A\bar{a}}^2\right)$$

$$\frac{d^4p_{B\bar{b}}}{(2\pi)^3} \delta^{(+)}\left(p_{B\bar{b}}^2 - m_{B\bar{b}}^2\right) \frac{d^4p_{\bar{C}c}}{(2\pi)^3} \delta^{(+)}\left(p_{\bar{C}c}^2 - m_{\bar{C}c}^2\right) \qquad (A.3)$$

$$\delta^{(+)}\left(p_d^2 - m_d^2\right) 2\pi \quad .$$

The absence of coherence in the decomposition can be physically motivated under the assumption that a, b are distinct "localized" constituents of A, B respectively. The ϕ's are the covariant vertex functions for one leg off-mass-shell. In the case of spin, the appropriate spin sums and traces are assumed. From the form of (A.2) and (A.3), we see that we are assuming that a, b, c, d have either well

defined masses (for internal hadrons) or effective masses (for quarks, etc.). These masses are later assumed to be small in some sense so that, for example, we do not include in (A.2) an internal $2 \to 3$ process where the effective mass of the system represented by d can be arbitrarily large.

It is convenient to choose the following parametrization

$$p_b^{(+)} \equiv p_b^0 + p_b^3 = x_b p_B^{(+)} ,$$
$$\vec{p}_{bT} = \vec{k}_{\bar{b}T} \qquad \vec{k}_{Tb} \cdot \vec{p}_B = 0 . \tag{A.4}$$

The mass-shell condition for $p_B - p_b$ then gives

$$(p_B - p_b)^2 = m_{B\bar{b}}^2 \tag{A.5}$$

and one easily finds

$$p_b^2 - m_b^2 = x_b \left[M_B^2 - \frac{\vec{k}_{Tb}^2 + m_{B\bar{b}}^2}{1 - x_b} - \frac{\vec{k}_{Tb}^2 + m_b^2}{x_b} \right] \tag{A.6}$$

and

$$\int \frac{d^4 p_{B\bar{b}}}{(2\pi)^3} \delta^{(+)}(p_{B\bar{b}}^2 - m_{B\bar{b}}^2) = \int \frac{d^2 k_{Tb}}{(2\pi)^3} \int_0^1 \frac{dx_b}{2(1 - x_b)} . \tag{A.7}$$

The limits on x_b ensure that $p_{B\bar{b}}$ is timelike and p_b is spacelike. We may then define the distribution

$$G_{b/B}(\vec{k}_{TB}, x_b) \equiv \frac{1}{(2\pi)^3} \frac{x_b}{2(1 - x_b)} \frac{\phi_B^2(p_b^2)}{(p_b^2 - m_b^2)^2} , \tag{A.8}$$

which is the probability for particle b to have fractional momentum $x_b = p_b^+ / p_B^+$ along the direction of particle B plus a transverse momentum $\vec{k}_{Tb}$ orthogonal to $\vec{p}_B$. The spectral sum over $m_{B\bar{b}}$ is understood in (A.8). The behavior $G_{b/B}$ at $x_b \sim 0$ is controlled by the behavior of the spectral integral at large $m_{B\bar{b}}^2$ which is, in turn, given by the high-s behavior of $\sigma_{B\bar{b}}(s)$. The existence of

$G_{b/B}$ implies that b can be "found" in the wave function of particle B and its use in the hard scattering formula means that it makes sense physically to distinguish between the formation of b in this way and the subsequent interactions of this off-mass-shell "constituent."

Similarly, we can define $G_{a/A}(\vec{k}_{Ta}, x_a)$ for the distribution of momenta carried by p_a in A where, again, p_a is spacelike. Finally, we also define

$$\begin{aligned} p_c^{(+)} &= y_c\, p_C^{(+)} \\ \vec{p}_{Tc} &= y_c \vec{p}_{TC} + \vec{k}_{Tc} \end{aligned} \quad . \tag{A.9}$$

where the mass shell condition for $p_c - p_C$ implies

$$p_c^2 - m_c^2 = y_c \left[m_C^2 + \frac{\vec{k}_{TC}^2 + m_{\overline{Cc}}^2}{y_c - 1} - \frac{\vec{k}_{TC}^2 + m_c^2}{y_c} \right] \tag{A.10}$$

and

$$\int \frac{d^4 p_{\overline{Cc}}}{(2\pi)^3}\, \delta^{(+)}(p_{\overline{Cc}}^2 - m_{\overline{Cc}}^2) = \int \frac{d^2 k_{TC}}{(2\pi)^3} \int_1^\infty \frac{dy_c}{2(y_c - 1)} \quad . \tag{A.11}$$

If we define $x_c = y_c^{-1}$, then the function

$$\tilde{G}_{C/c}(x_c, \vec{k}_{TC}) = \frac{1}{(2\pi)^3} \frac{1}{2(x_c^{-1} - 1)} \frac{\phi_c^2(p_c^2)}{(p_c^2 - m_c^2)^2} \tag{A.12}$$

gives the probability, normalized to the multiplicity, for particle C to have a fraction x_c of the momentum along the direction of the timelike particle c and a component $\vec{k}_{TC}$ normal to this direction. The tilde indicates the parent particle c is timelike.

Without further approximation we may then write Eq. (A. 1) in the form

$$\frac{d\sigma(AB \to CX)}{d^3p_C/E_c} = \sum_{ab,\,cd} \int d^2k_{Ta} \int_0^1 dx_a \int d^2k_{Tb} \int_0^1 dx_b \int d^2k_{TC} \int_0^1 \left(\frac{dx_c}{x_c^2}\right)$$

$$G_{a/A}(\vec{k}_{Ta}, x_a)\, G_{b/B}(\vec{k}_{Tb}, x_b)\, \tilde{G}_{C/c}(\vec{k}_{TC}, x_c) \qquad (A.13)$$

$$\left(\frac{1}{x_a x_b 2E_a 2E_B}\right)\left(\frac{1}{|V_A - V_B|}\right) |M_{ab\to cd}|^2 \frac{\delta_{(+)}(p_d^2 - m_d^2)}{(2\pi)^3} \,.$$

The next step is to assume that the off-shell continuations in the integrand of (A.13) are not important so that we can identify

$$\frac{1}{x_a x_b 2E_a 2E_b} \frac{1}{|V_A - V_B|} |M_{ab\to cd}|^2 \frac{1}{(2\pi)^2} = \frac{s'}{\pi} \frac{d\sigma(ab \to cd)}{dt'}\bigg|_{s't'u'}$$

and (A.14)

$$\delta_{(+)}(p_d^2 - m_d^2) \cong \delta(s' + t' + u' - m_a^2 - m_b^2 - m_c^2 - m_d^2)$$

where

$$\begin{aligned} s' &= (p_a + p_b)^2 \cong x_a x_b s - \vec{k}_{Ta}\cdot\vec{k}_{Tb} \\ t' &= (p_a - p_c)^2 \cong \frac{x_a}{x_c} t + \vec{k}_{Ta}\cdot\vec{k}_{TC} \\ u' &= (p_b - p_c)^2 \cong \frac{x_b}{x_c} u + \vec{k}_{Tb}\cdot\vec{k}_{TC} \end{aligned} \qquad (A.15)$$

when the masses m_a^2, m_b^2, m_c^2, m_d^2 can be neglected.

The next assumption is that the structure functions

$$G_{a/A}(x) = \int d^2\vec{k}_T \; G_{a/A}(\vec{k}_T, x) \qquad (A.16)$$

exist. Note, from (A.8) and (A.12) that the integrals converge even for ϕ = constant.

We then write, with $s', t' >> \vec{k}_T^2$

$$\frac{d\sigma(AB \to CX)}{d^3p_c/E_c} \cong \sum_{ab,\,cd} \int_0^1 dx_a \int_0^1 dx_b \int_0^1 \frac{dx_c}{x_c^2}\, G_{a/A}(x_a)\, G_{b/B}(x_b)$$
$$\tilde{G}_{C/c}(x_c)\, \delta(s' + t' + u')\, \frac{s'}{\pi}\, \frac{d\sigma}{dt'}(ab \to cd)\,. \tag{A.17}$$

Comparing (A.8) and (A.12) assuming that $\phi^2(p_c^2)$ can be defined for both space-like and timelike arguments, we get

$$G_{c/C}(x) = -x\, \tilde{G}_{C/c}(1/x) \tag{A.18}$$

which is the crossing relation discussed in Section IV. This result, combined with

$$G_{\bar{c}/\bar{C}}(x) = G_{c/C}(x) \tag{A.19}$$

gives the correct crossing behavior for $AB \to CX$ to continue to $\bar{C}A \to \bar{B}X$. In In the case where c and C consist of a boson and a fermion, there is an extra sign reversal in (A.18).

APPENDIX B

RELATION BETWEEN CALCULATIONAL TECHNIQUES

An often perplexing feature of theoretical papers on large transverse momentum is the number of diverse, yet equivalent calculational techniques. Various authors use Bethe-Salpeter, Fock-space methods, or integral representations of scattering amplitudes to represent bound state amplitudes, and either Sudakov variables, light-cone variables, infinite momentum frame parametrizations, or standard Feynman variables to parametrize integrals. In this appendix we will discuss some of the interrelations among these techniques. Further details may be found in a paper by M. Schmidt (1974). (See also Brodsky, Close and Gunion, 1973.)

A convenient illustration of the various methods is the calculation of hadronic form factors, particularly the normalization integral since it provides a simple method to define the structure function and to relate it to a quark parton scattering amplitude.

The form factor (assuming only spinless particles are involved) corresponding to Fig. B.1a is defined by

$$(2p+q)^{\mu} F(q^2) = \int \frac{d^4k_i}{(2\pi)^4} \frac{(2k+q)^{\mu} T(p, k+q \to p+q, k)}{(k^2 - M^2 + i\epsilon)\,((k+q)^2 - M^2 + i\epsilon} \quad . \tag{B.1}$$

The relation to the off-shell scattering amplitude is indicated in Fig. B.1b. Self energy insertions can also be included readily in this model.

Although the standard Feynman parametrization is useful for specific forms for T, in general it is more useful to try to reduce the k-integration. Among the many possible parametrization are

(a) Sudakov: $k = xp + yq + n, \quad n \cdot q = n \cdot p = 0 \, .$ (B.2)

(b) Light-cone: $k^+ = k^0+k^3 = x(p^0+p^3)$, $k^- = k^0-k^3 = \dfrac{\vec{k}_T^2 + k^2}{k^+}$ (B.3)

where p is taken in the z-direction and $q^+ = 0$.

(c) Infinite momentum: one chooses

$$p = \left(P + \frac{M^2}{2P},\ \vec{O}_T,\ P\right)$$
$$k = \left(xP + \frac{k^2 + \vec{k}_T^2}{2xP},\ \vec{k}_T,\ xP\right) \qquad \text{(B.4)}$$

where

$$P^2 \gg M^2,\ k^2,\ \vec{k}_T^2 \ .$$

Note that the light cone parametrization is exactly equivalent to the choice of frame

$$p = \left(P + \frac{M^2}{4P},\ O_T,\ P - \frac{M^2}{4P}\right)$$
$$k = \left(xP + \frac{k^2 + \vec{k}_T^2}{4xP},\ \vec{k}_T,\ xP - \frac{\vec{k}_T^2}{4xP}\right) \qquad \text{(B.5)}$$

where P may now be chosen arbitrarily. In fact $Y = \log\frac{2P}{M}$ is the rapidity of p relative to the rest frame $2P = M$. Also, $y = \log x$ is the rapidity of k relative to p. Note that y is often a useful variable, especially in multiperipheral calculations making the phase space integral $\int dx/x = \int dy$ uniform in rapidity. If $P \to \infty$, we have exactly the infinite momentum frame, where $x \Rightarrow k_z/p_z$ becomes the fractional longitudinal momentum.

In order to proceed further, it is convenient to assume that T can be written as a sum over its u-channel singularities (see Fig. B.1c). Thus

$$T = \int \rho(\sigma^2)\ \frac{\phi_\sigma(k^2)\,\phi_\sigma[(k+q)^2]}{(p-k)^2 - \sigma^2}\ d\sigma^2 \ . \qquad \text{(B.6)}$$

This can be done in various ways; for example by assuming a dispersion relation, or choosing a suitable integral representation. We then have for any of

the variable choices (b) $\longleftrightarrow$ (d),

$$\int d^4k = \int d^4(p-k) = \int d^2k_T \int \frac{dx}{2(1-x)} \int d(p-k)^2 \tag{B.7}$$

with

$$k^2 - m_q^2 = xS(\vec{k}_T, x)$$

$$(k+q)^2 - m_q^2 = x\tilde{S} = xS(\vec{k}_T + (1-x)\vec{q}_T, x) \tag{B.8}$$

and we have defined

$$S(\vec{k}_T, x) = M^2 - \frac{\vec{k}_T^2 + m_q^2}{x} - \frac{\vec{k}_T^2 + \sigma^2}{1-x} \quad . \tag{B.9}$$

If $x > 0$ or $x < 1$, then all of the singularities in $(p-k)^2$ are in the upper half plane and there is no contribution. For $0 < x < 1$, we can close the contour in the lower half plane and pick up the $(p-k)^2 - \sigma^2$ pole, and obtain (using the $p_0 + p_3$ component)

$$F(q^2) = \int \frac{d^2k_T}{(2\pi)^3} \int_0^1 \frac{dx}{2(1-x)} x \int d\sigma^2 \frac{\phi_\sigma(x,S)}{xS} \frac{\phi_\sigma(x,\tilde{S})}{x\tilde{S}} \rho(\sigma^2) \, . \tag{B.10}$$

For a given single particle contribution to $\rho(\sigma^2)$, ϕ_σ can be identified with the Bethe-Salpeter wavefunction with one-leg on shell

$$\lim_{(p-k)^2 - \sigma^2 = 0} \left[(p-k)^2 - \sigma^2\right] \psi\left(k^2, (1-k)^2\right) = \phi_\sigma(k^2) \, . \tag{B.11}$$

Alternately, we can use Fock space wavefunctions in the $P \to \infty$ frame, and identify

$$\psi_{P \to \infty}(\vec{k}_T, x) = \frac{\phi_\sigma(xS)}{S} \, . \tag{B.12}$$

Parallel results are also obtained using the Sudakov variables by using the $(p-k)^2$ pole to do the y integrations (Landshoff and Polkinghorne, 1972b).

Since $F(0) = 1$, we can define

$$F(x) = G_{a/p}(x) = \int \frac{d^2k_T}{2(1-x)(2\pi)^3} \int d\sigma^2 \, \frac{\phi_\sigma^2(xS)}{(xS)^2} \, x \tag{B.13}$$

as the normalized fractional momentum distribution. Note that x can be interpreted variously according to the parametrization (a) → (d) used above. It is easy to see that the "handbag" diagram, Fig. B.1d, for forward virtual Compton scattering gives

$$\nu W_2(x) = \sum_a \lambda_a^2 \, x f_a(x) \Big|_{x=\omega=1} \tag{B.14}$$

where λ_a is the constituent charge.

Finally, we can also identify $\phi_\sigma^2(k^2)$ with the u-channel discontinuity of the virtual forward scattering amplitude $T(k, p \to k, p)$. Thus we have

$$\nu W_2(x) = x \sum_a \lambda_a^2 \, \frac{1}{2x(1-x)} \int \frac{d^2k_T}{(2\pi)^3} \int d\sigma^2 \, \frac{\mathrm{Im}_u T(x, S, \sigma^2)}{S^2} \tag{B.15}$$

which is the important relation obtained by Landshoff and Polkinghorne (1972). It is easy to see that if $\sigma_{\overline{a}p} \sim s^\alpha$, $\alpha > 0$, then $\mathrm{Im}\, T \sim (\sigma^2)^{\alpha-1}$ and $\nu W_2(x) \sim x^{1-\alpha}$ at $x \to 0$.

APPENDIX C

CALCULATIONS OF WIDE-ANGLE SCATTERING AMPLITUDES

One of the simplest techniques for calculating scattering amplitudes for composite systems is the "partition" method; i. e.: the effective replacement of each hadron by constituents carrying finite fractions of the hadronic momentum. This is justified as follows: by definition the hadronic amplitude is given by the convolution of hadronic wave functions and n-particle amplitude integrated over relative momentum $k^{\mu}(i)$

$$M_{A + B \to C + D} = \int \psi^{\dagger C}_{BS} \psi^{\dagger D}_{BS} M_n \psi^{A}_{BS} \psi^{B}_{BS} \prod_i d^4 k_i . \qquad (C.1)$$

Assuming finite hadronic binding; i. e.: finite Bethe-Salpeter wavefunctions at relative $x^{\mu} = 0$, the leading contribution at large t and u can be obtained explicitly by iterating the kernel where ever large relative momentum are required. Thus all the wavefunctions are evaluated in their natural domain of near on-shell constituents, e. g. $p_a = x_a P_A + k_A$, with $0 < x_a < 1$, $k_a \cdot p = 0$, and k_A^2 small , and all of the hard momenta is exchanged within M_n.

Some representative contributions to M_n for meson-meson scattering are shown in Fig. C.1. (Note that all of these contributions except (c) occur in positronium-positronium scattering.)

It is easy to check that each of the graphs (a)-(d) scale at fixed θ_{cm} as s^{-2} in any renormalizable theory. In these Born graphs, only the off-shell quark propagators need be counted to obtain the scaling behavior, as in ϕ^4 theory; otherwise the gluon propagator fall-off is compensated by the vertex couplings — from the convection current for spinless quarks or from the trace in the spin $\frac{1}{2}$ case. Additional, but finite, powers of log s factors appear from the $x \sim 1$ integrations, corresponding to degeneracy of routings of the large momentum transfer.

Diagram (a) is the prototype of the Wu-Yang gluon exchange model, which has been generalized by Abarbanel, Drell, and Gilman (1969), Fried, Gaisser, and Kirby (1970, 1973), and by Horne and Moshe (1973). Following the latter authors, we can generalize such contributions to the form

$$M_{A+B\to C+D} = F_{AC}(t)\, M_{quark}(s,t)\, F_{BD}(t) + \text{crossing contributions} \quad . \tag{C.2}$$

If vector or axial-vector gluon exchanges are involved then this gives Regge behavior $M \sim s^{\alpha(t)}\beta(t)$ $(s \gg t)$ with $\alpha(t) \sim 1$ for all t. The phenomenological difficulties with this form are reviewed in Section V. Note that Fig. C.1b gives a contribution $\sim t^{-2}$; i. e.: $\alpha(t) = 0$, but is not usually taken into account in such models. We also emphasize that if gluon exchange is allowed in a composite model, then the Landshoff (1974b) contributions which we discuss below and in Section IVC dominate the fixed angle amplitude so the above theories are the most consistent representation of the asymptotic amplitude. (Note, however, that in some elementary vector gluon field theory models, the Landshoff contributions cancel. See Halliday, Huskins and Sachrajda (1974a, b).) Figure C. 1e contains the double-scattering (Landshoff) contribution. The matrix element scales as $is^{-3/2}$, and is dominated by the on mass shell region with $1-x_a \sim x_b \sim 1-x_c \sim x_d$. In general, higher order loop contributions to M_n introduce additional powers of log s in each order in perturbation theory. In accordance with Bjorken scaling, or from the various theoretical arguments advanced in Section IV, it is assumed that these logarithms do not accumulate to change the overall power indicated by the lowest order contributions.

Diagrams (c) and (d) are the prototypes of the constituent interchange model, giving contributions to meson-meson scattering that survive even if gluon exchange between quarks of different hadrons are excluded. Independent of the

gluon or constitutent spin, one obtains the contributions

$$M_{(c)} \sim \frac{1}{u}\frac{1}{t} , \qquad M_{(d)} \sim \frac{1}{s}\frac{1}{t} \tag{C.3}$$

(modulo logarithms from the $x \sim 1$ integrations), and thus a Regge contribution at $\alpha = -1$. A natural generalization of this result for $M_{(c)}$ to meson-baryon and baryon-baryon scattering, as adopted in the original CIM paper is

$$M_{CIM}^{A + B \to C + D} = u F_A(u) F_C(u) F_D(t) . \tag{C.4}$$

This form can be justified if each composite system is effectively treated as a bound state of two particles; in particular, the proton must be regarded as a quark + core (or diquark) bound state. Using Eq. (C.4) we have the interchange model prediction

$$M_{MB \to MB} \sim \alpha \frac{1}{u}\frac{1}{t^2} + \beta \frac{1}{s}\frac{1}{t^2} , \qquad \text{i.e.} \quad \alpha(t) \Rightarrow -1 \tag{C.5}$$

for the quark and antiquark contributions and

$$M_{BB \to BB} \sim \frac{1}{u^3}\frac{1}{t^2} , \qquad \text{i.e.:} \quad \alpha(t) \Rightarrow -3 \tag{C.6}$$

for the quark interchange contribution to baryon-baryon scattering in the core model. Inclusion of spin changes this result slightly. The proton core model is attractive in that (1) it can naturally account for the anomalous behavior of $\nu W_2^p / \nu W_2^n$ at $x \to 1$, and (2) the spectroscopy of baryon resonances seems to favor a diquark-quark model. The diquark state is predicted to be quasi-stable in color models (see e.g. Capps, 1974). Further discussion of the use of the core model has been given by Gunion (1974). Note that (C.6) predicts $d\sigma/dt\ (pp \to pp) \sim s^{-12} (1 - \cos^2\theta_{cm})^{-n}$ with $n \sim 6$ which gives a good representation of the large angle data. The prediction

$$d\sigma/dt\ (K^+ p \to K^+ p) \sim s^{-8} (1 - \cos\theta)^{-4} (1 + \cos\theta)^{-1} \tag{C.7}$$

from Eq. (C.5) (including an extra factor of $(1+\cos\theta)^1$ from a helicity-conservation) due to p-quark interchange gives an excellent representation of the k^+p data. The core model can be simulated using a super-renormalizable field theory model for the proton couplings.

An even more convenient generalization of (C.4) for the interchange model which can be used for the case of a three quark baryon system for a ut graph is

$$M^{CIM}_{A+B\to C+D}(u,t) = M_{q+A\to q+A}(u,t)\, F_{BD}(t) \qquad (C.8)$$

where $F_{BD}(t)$ is assumed to be the most convergent form factor. The quark amplitude is evaluated at the appropriate kinematics. This form, which easily follows from the structure of Fig. C.1 , is discussed in detail in Section V.A and is consistent with the dimensional counting rules for a three quark wave function. Logarithms from the $x \sim 1$ integration are autormatically included.

The fact that different results for the CIM model can be obtained for different choices of the hadronic wavefunction was emphasized by Fishbane and Muzinich (1973). It is easy to check that this ambiguity only occurs for baryon-baryon scattering and is resolved once the basic quark-core or three quark structure is assumed.

APPENDIX D

ALTERNATIVE THEORIES BASED ON PARTON INTERCHANGE

During the past year, several other models of large angle scattering processes based on duality or "urbaryon" (i. e. : quark) rearrangement diagrams have been developed. The essential forms and assumptions used in these models are similar to those of the CIM, although there are important differences.

An interesting though heuristic formula for large angle two body exclusive processes $A + B \rightarrow C + D$ has been proposed by Kinoshita and his coworkers (1974a, b): for large t and u they propose

$$M \sim \frac{1}{s^{N_S}} \frac{1}{t^{N_T-1}} \frac{1}{u^{N_U-1}}$$

$$\frac{d\sigma}{dt} = \frac{1}{s^N} (1-z)^{2-2N_T} (1+z)^{2-n_U} \qquad \text{(D. 1)}$$

where n_T is the total number of "bonds" connecting the hadrons in the t-channel (i. e. : the total number of quark lines connecting A to C or B to D), etc. The overall power law agrees with dimensional counting rule $N = N_A + N_B + N_C + N_D - 2$. Although the angular dependence is derived heuristically, its form reflects the tendency of the valence quarks to persist in their direction of motion. In terms of Regge behavior, for $s >> -t$, one has

$$\alpha_{eff}(t) = 1 - (n_S + n_U)\, \gamma(-t) \qquad \text{(D. 2)}$$

where $\gamma(-t) \rightarrow 1$ for large negative t. Unlike Eq. (C.5) $\alpha(-\infty)$ only depends on the number of exchanged quarks. Note, also that Eq. (D.1) is <u>not</u> in general consistent with crossing symmetry. For pp scattering, single quark interchange gives ($n_S = 0$, $n_T = 4$, $n_U = 2$)

$$s^{10}\frac{d\sigma}{dt} \sim (1-z)^{-6}(1+z)^{-2}, \quad \alpha(t) \to -1 \tag{D.3}$$

and double quark interchange (as required ty t-u crossing)

$$s^{10}\frac{d\sigma}{dt} \sim (1-z)^{-2}(1+z)^{-6}, \quad \alpha(t) \to -3 \tag{D.4}$$

compared with $\alpha(t) \to -2$ for the CIM using Eq. (VD.2). A novel feature of Eq. (D.1) is that the "diffractive" term with zero quark exchange ($n_S = 0$, $n_T = 6$, $n_U = 0$) gives automatically an $\alpha_{eff}(t) = 1$ contribution. Kinoshita and Myozyo (1974) use the sum of the above three contributions (interference and spin effects, and the u-channel diffractive term are ignored) to give a fairly good parametrization of the pp data. The small t dependence of $\gamma(t)$ can be chosen to give backward peaks (which vanish in the fixed-angle scattering limit) in K^-p and p^-p elastic reactions. A troubling feature of the suggested rule is that all $n_U = 0$ contributions vanish strongly in the backward direction in the scaling limit.

An alternative approach to the calculation of u baryon rearrangement diagrams is given by Igarashi, Nishitani, Matsuoa, and Swada (1974). These authors propose the fixed angle scaling law

$$M = \frac{1}{s^{N_S-1}}\frac{1}{t^{N_T}}\frac{1}{u^{N_U}}$$

$$\frac{d\sigma}{dt} = \frac{C}{s^{N_{TOT}}}(1-z)^{-2n_T}(1+z)^{-2n_U} \tag{D.5}$$

which differs from (D.1) by a factor of $p_T^{-4} = (tu/s)^{-2}$ in the cross section. Here N_{TOT} is the total number of fields in A, B, C, D; thus the predictions fall two powers of s faster than those based on dimensional counting, and due to mass corrections, present data must be assumed to be subasymptotic. The proposed

effective trajectory $\alpha_{eff}(-t) \rightarrow -3$ power-law dependence s^{-12} for pp scattering, and phenomenological treatment of the diffractive amplitude are essentially the same as the CIM using the quark plus core model. The predictions differ for other channels, however. Again, we note the absence of crossing symmetry in the proposed rule.

Because of the freedom of mass terms, and the freedom of choice of the trajectories at lower t, a successful phenomenology of two body reactions can be based on the CIM predictions or either (D.1) or (D.5). The most decisive test will be an accurate experimental determination of the asymptotic power dependence of pp → pp. It should be emphasized that data for a large but fixed cm angular range can be used for this purpose.

Kinoshita et al. have also proposed a set of counting rules for inclusive large p_T reactions based upon u baryon rearrangement diagrams. As in the CIM, the results displaying a continuity of physics throughout the Peyrou plot, giving connections between large p_T phenomena and the triple and central Regge region of exclusive processes. However, the proposed counting rules do not recognize the importance of the subprocess in determining the p_T^2 fall-off, and the predicted powers at fixed t/s, $\mathcal{M}^2/s$ seem unreasonable (e.g. p_T^{-2} for $\gamma B \rightarrow MX$, p_T^{-4} for $MB \rightarrow MX$, whereas p_T^{-8} for $BB \rightarrow BX$, $BB \rightarrow MX$).

LIST OF FIGURES FOR THE APPENDICES

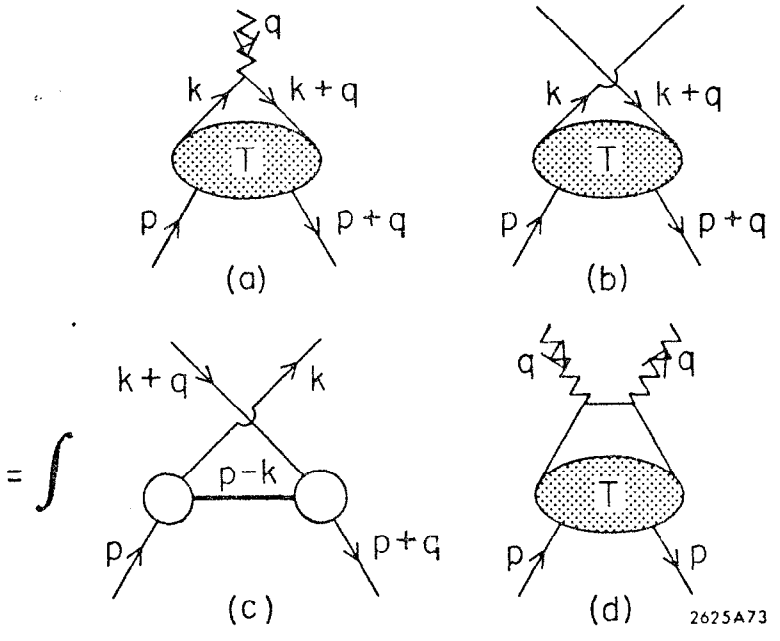

FIG. B.1

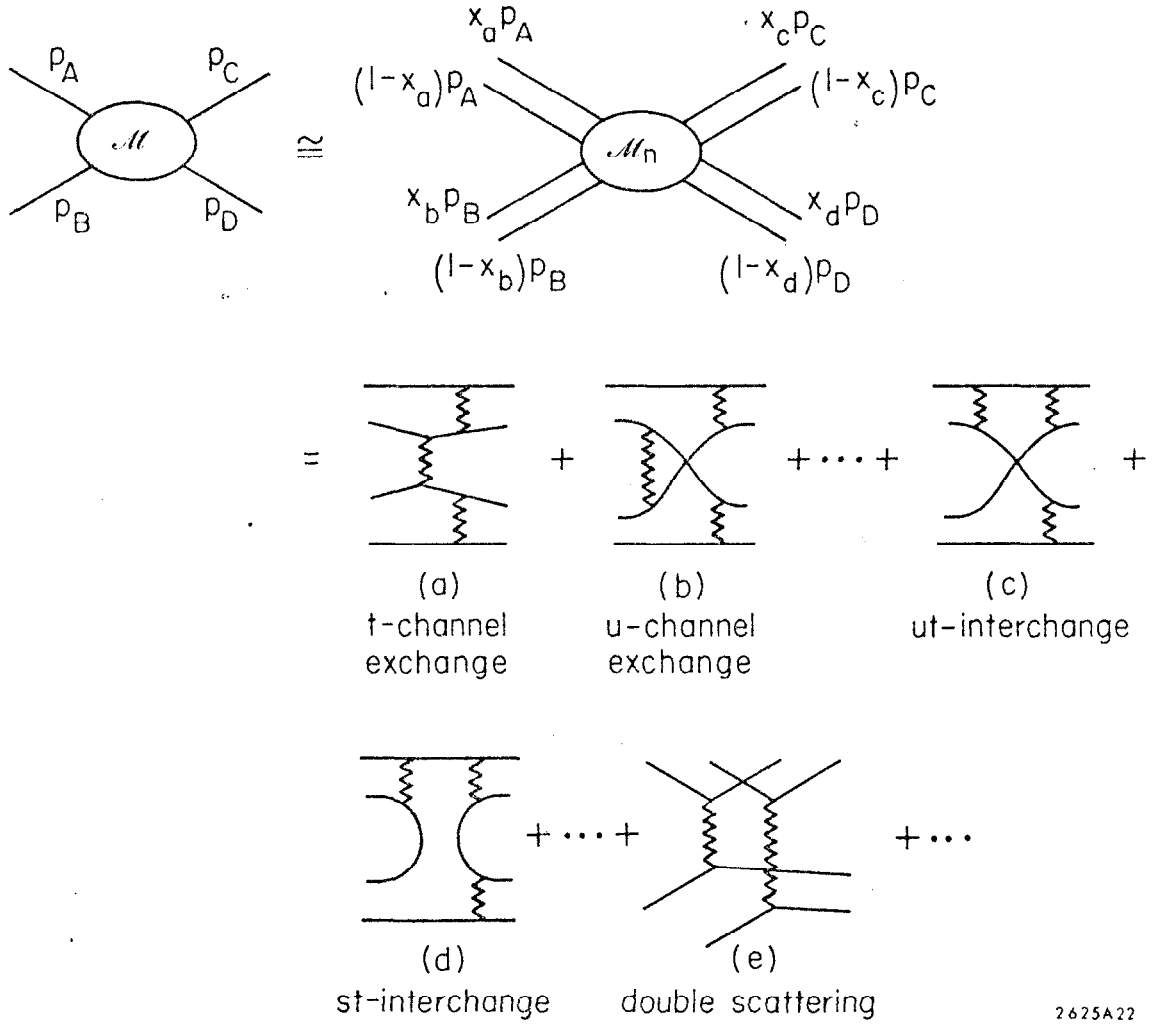
p_A
p_C
$\mathcal{M}$
p_B
p_D
$\cong$
$x_a p_A$
$(1-x_a)p_A$
$x_b p_B$
$(1-x_b)p_B$
$\mathcal{M}_n$
$x_c p_C$
$(1-x_c)p_C$
$x_d p_D$
$(1-x_d)p_D$
=
+
+ ··· +
+
(a)
t-channel
exchange
(b)
u-channel
exchange
(c)
ut-interchange
+ ··· +
+ ···
(d)
st-interchange
(e)
double scattering
2625A22

FIG. C.1

REFERENCES

Abarbanel, H., S. Drell, F. Gilman (1969), Phys. Rev. 177, 2458

Abshire, G. W. et al. (1974), Phys. Rev. D 9, 555

Akerlof, C. W. et al. (1967), Phys. Rev. 159, 1138

Alabiso, C. and G. Schierholz (1974), Phys. Rev. D 10, 960

Allaby, J. V. et al. (1966), Phys. Letters 23, 384

Alonso, J. and D. Wright (1975), SLAC-PUB-1578

Alper, B. et al. (1973), Phys. Letters 47B, 75

_____ (1974a), Nuovo Cimento Letters 11, 173

_____ (1974b), CERN PRINT-74-1659

Amati, D., L. Caneschi and M. Testa (1973), Phys. Letters 43B, 186

Anderson, E. W. et al. (1974), BNL-19236

Appel, J. A. et al. (1974a), Phys. Rev. Letters 33, 719

_____ (1974b), Phys. Rev. Letters 33, 722

Appelquist, T., S. Coleman and H. Quinn (1974), private communication

Appelquist, T. and E. Poggio (1974), Harvard preprint

Appelquist, T. and J. Primack (1970), Phys. Rev. D 1, 1144

Aubert, J. J. et al. (1974), Phys. Rev. Letters 33, 1404

Augustin, J. E. et al. (1974), Phys. Rev. Letters 33, 1406

Baglin, C. et al. (1973a), Phys. Letters 47B, 85

_____ (1973b), Phys. Letters 47B, 89

Baker, M. and D. Coon (1971), Phys. Rev. D 4, 1234

Bander, M., R. M. Barnett and D. Silverman (1974), Phys. Letters 48B, 243

Banner, M. et al. (1973), Phys. Letters 44B, 537

Bardeen, W., M. Chanowitz, S. Drell, M. Weinstein, and Y.-M. Yan (1974), SLAC-PUB-1490

Barger, V., F. Halzen and J. Luthe (1972), Phys. Letters 42B, 428

Barnett, R. and D. Silverman (1974), Phys. Rev. D 10, 1510

Berger, E. L. and D. Branson (1973), Phys. Letters 45B, 57

Berman, S. M., J. D. Bjorken and J. B. Kogut (1971), Phys. Rev. D 4, 3388

Berman, S. M. and M. Jacob (1970), Phys. Rev. Letters 25, 1683

Berman, S. M., D. J. Levy and T. L. Neff (1969), Phys. Rev. Letters 23, 1363

Betev, B. et al. (1974), CERN PRINT-75-0019

Bjorken, J. D. (1973a), Phys. Rev. D 8, 4098

_____ (1973b), Proc. of the SLAC Institute on Particle Physics, Vol. I, edited by M. Zipf

_____ (1973c), Talk presented at Aix-en-Provence International Conference on Elementary Physics

_____ (1974), Acta Physica Polonica B5, 893

Bjorken, J. D. and J. Kogut (1973), Phys. Rev. D 8, 1371

Bjorken, J. D. and E. Paschos (1969), Phys. Rev. 185, 1975

Blankenbecler, R. (1972), Proc. of the Canadian Inst. of Particle Physics, McGill

_____ (1974), Talk presented at the IXth Balaton Symposium on Particle Physics

Blankenbecler, R. and S. Brodsky (1974), Phys. Rev. D 10, 2973

Blankenbecler, R., S. J. Brodsky and J. F. Gunion (1972a), Phys. Letters 39B, 649

_____ (1972b), Phys. Rev. D 6, 2652

_____ (1973), Phys. Letters 42B, 461

_____ (1975), SLAC-PUB-1585

Blankenbecler, R., S. J. Brodsky, R. Savit, and J. Gunion (1973), Phys. Rev. D 8, 4117

_____ (1974), Phys. Rev. D 10, 2153

Blankenbecler, R., J. Tran Thanh Van, J. F. Gunion, and D. Coon (1974), SLAC-PUB-1483

Bloom, E. D. and F. J. Gilman (1970), Phys. Rev. Letters 25, 1140

Bohm, M. and M. Krammer (1974), Phys. Letters 50B, 457

Bonneau, G. et al. (1974), CERN PRINT-74-0986

Borenstein, J. M. (1975), Harvard preprint

Borghini, M. et al. (1967), Phys. Letters 24B, 77

_____ (1971), Phys. Letters 36B, 500

Bouquet, A., J. Letessier and A. Tounsi (1974), Phys. Letters 51B, 235

Boyarski, A. M. et al. (1974), to be published

Boymond, J. P. et al. (1974), Phys. Rev. Letters 33, 112

Brockett, W. S. et al. (1974), Phys. Letters 51B, 390

Brodsky, S. (1973), in High Energy Collisions, edited by C. Quigg (American Institute of Physics, New York)

_____ (1974a), SLAC Summer Institute of Particle Physics, Vol. II SLAC-179

_____ (1974b), Invited Talk, Int. Conference on Few Body Problems in Nuclear and Particle Physics, Quebec, Canada

Brodsky, S., F. Close and J. Gunion (1973), Phys. Rev. D 8, 3678

Brodsky, S. and G. Farrar (1973), Phys. Rev. Letters 31, 1153

_____ (1975), Phys. Rev. D 11, 1309

Brodsky, S., J. Gunion and R. Jaffe (1972), Phys. Rev. D 6, 2487

Buran, T. et al. (1974), CERN preprint

Busser, F. W. et al. (1973), Phys. Letters 46B, 471

_____ (1974), Phys. Letters 51B, 306

Cahalan, R. F., K. A. Geer, J. Kogut, and L. Susskind (1974), Cornell University preprint CLNS-289

Callan, C. G. and D. J. Gross (1974), Princeton University preprint

Capps, R. (1974), Purdue preprint

Carey, D. C. et al. (1974a), Phys. Rev. Letters 32, 24

_____ (1974b), Phys. Rev. Letters 33, 327

Casher, A., J. Kogut and L. Susskind (1974), Phys. Rev. D 10, 732

Carruthers, P. and M. Duong-Van (1973), Phys. Rev. Letters 21, 133

Cerulus, F. and A. Martin (1964), Phys. Letters 8, 80

Chen, M. C., Ling-Lie Wang and T. F. Wong (1972), Phys. Rev. D 5, 1667

Chen, M. C. and P. Zerwas (1974), SLAC-PUB-1492

Chiu, C. (1972), Texas preprint (unpublished)

Chodos, A. et al. (1974a), Phys. Rev. D 9, 3471

_____ (1974b), Phys. Rev. D 10, 2559

Christenson, J. et al. (1970), Phys. Rev. Letters 25, 1523

_____ (1973), Phys. Rev. D 8, 2016

Chu, S.-Y. and A. W. Hendry (1972), Phys. Rev. D 6, 190

_____ (1973), Phys. Rev. D 7, 86

Ciafaloni, M. and S. Ferrara (1974), Scuola Normale Superiore, Pisa preprint 16

Clifford, T. S. et al. (1974), Phys. Rev. Letters 33, 1239

Contogouris, A., J. Holden and E. Argyres (1974), Phys. Letters B51, 25

Coon, D. (1974), University of Pittsburgh preprint PITT-125

Cornwall, J. M., D. Corrigan and R. E. Norton (1971), Phys. Rev. D 3, 536

Cottrell, R. et al. (1975), Phys. Letters 55B, 341

Creutz, M. and L.-L. Wang (1974), BNL-19078

Cronin, J. W. (1974), Proc. of the 1974 Summer Institute of Particle Physics, Vol. II, SLAC-179, p. 279

Cronin, J. W. et al. (1973), Phys. Rev. Letters 31, 1426

Cronin, J. W. et al. (1974), Chicago EFI preprints 74-1181 and 74-1182

Cvitanovic, P. (1974), Phys. Rev. D 10, 338

Danysz, P. et al. (1972), Nucl. Phys. B42, 29

Darriulat, P. et al. (1974), CERN PRINT-75-0019

Del Prete, T. (1974), Invited Talk given at IXth Balaton Symposium on Particle Physics, Balatonfured, Hungary, 1974; CERN preprint

DeTar, C. et al. (1971), Phys. Rev. D 4, 425

Donnachie, A. and P. R. Thomas (1974), Daresbury preprint DL/P220, submitted to Nuovo Cimento

Drell, S. D. and T.-M. Yan (1970), Phys. Rev. Letters 24, 181

_____ (1971), Ann. Phys. (N.Y.) 66, 578

Dumont, J. J. and L. Heiko (1974), Brussels preprint IIHE-74-1

Eide, A. et al. (1973), Nucl. Phys. B60, 173

Eilam, G. et al. (1973), Phys. Rev. D 8, 2871

Eisner, A. M. et al. (1974), Phys. Rev. Letters 33, 865

Ellis, S. D. (1974a), Phys. Letters 49B, 189

Ellis, S. D. (1974b), XVII Int. Conference on High Energy Physics, London

Ellis, S. D. and P.G.O. Freund (1970), NAL-THY 82, unpublished

Ellis, S. D. and M. B. Kislinger (1974), Phys. Rev. D 9, 2027

Ellis, S. D. and R. Thun (1974), CERN preprint TH-1874

Elvekjaer, F. et al. (1973), Nucl. Phys. B64, 301

Ericson, T.E.O. (1963), Ann. Phys. (N.Y.) 23, 390

Ezawa, Z. F. (1974), Nuovo Cimento 23A, 271

Ezawa, Z. F. and K. Nishijima (1972), Prog. Theor. Phys. 48, 1751

Ezawa, Z. F. and J. C. Polkinghorne (1974), University of Cambridge preprint DAMTP 74/20

Farrar, G. (1974), Nucl. Phys. B77, 429

Farrar, G. and C. C. Wu (1974), CALT-68-455

Feynman, R. P. (1972), Photon-Hadron Interactions (W. A. Benjamin, Inc., Reading, Massachusetts)

Finnocchiaro, G. et al. (1974), Phys. Letters 50B, 396

Fishbane, P. and I. Muzinich (1973), Phys. Rev. D 8, 4015

Frautschi, S. (1971), Phys. Rev. D 3, 2821

_____ (1972), Nuovo Cimento 12A, 133

Fried, H. M. (1974), Phys. Letters 51B, 90

Fried, H., T. K. Gaisser (1973), Phys. Rev. D 7, 741

Fried, H., T. K. Gaisser and B. Kirby (1970), Phys. Rev. Letters 25, 625

_____ (1971), Phys. Rev. D 4, 2220

_____ (1972), Phys. Rev. D 6, 2560

_____ (1973a), Phys. Rev. D 8, 2668

_____ (1973b), Phys. Rev. D 8, 3210

Goldberger, M. and F. Low (1968), Phys. Rev. 176, 1778

Gourdin, M. (1974), Phys. Reports

Gribov, V. N. and L. V. Lipatov (1972), Sov. J. Nucl. Phys. 15, 438

Gunion, J. (1974a), Phys. Rev. D 10, 242

_____ (1974b), Proc. APS Div. Particles and Fields

_____ (1974c), Proc. XVII Int. Conference on High Energy Physics

Hagedorn, R. (1968), Nuovo Cimento 56A, 1027

Hagedorn, R. and J. Ranft (1968), Nuovo Cimento Supplemento 6, 109

Halliday, J. G. and J. Huskins (1975), ICTP/74/4

Halliday, J. G., J. Huskins and C. T. Sachrajda (1974a), Nucl. Phys. B83, 189

_____ (1974b), Nucl. Phys. B87, 93

Harte, J. (1969), Phys. Rev. 184, 1948

_____ (1972), Nucl. Phys. B50, 301

Hayasyi, K. and H. Yabuki (1974), Kyoto University preprint RIMS-175

Heiko, L. (1974), Louvain preprint, unpublished

Hendry, A. (1974), Phys. Rev. D 10, 2300

Hendry, A. W. and G. W. Abshire (1974),

Horn, D. and M. Moshe (1973), Nucl. Phys. B57, 139

Igarashi, Y., T. Matsuoka and S. Sawada (1974), Prog. Theor. Phys. 52, 618

Hwa, R. C. and C. S. Lam (1971), Phys. Rev. Letters 27, 1098

Jabs, Arthur (1974), Nuovo Cimento Letters 9, 570

Jackiw, R. (1968), Ann. Phys. 48, 292

_____ (1969), Ann. Phys. 51, 575

Jacob, M. (1974), CERN preprint TH. 1453

Jacob, M. and R. Slansky (1972), Phys. Rev. D 5, 1847

Jaffe, R. L. (1974), MIT preprint CTP-448

Jain, P. L. et al. (1974), Phys. Rev. Letters 32, 797

Kane, G. (1974), Proc. XVII Int. Conference on High Energy Physics

Kinoshita, K. (1964), Phys. Rev. Letters 12, 257

_____ (1974), Prog. Theor. Phys. 51, 1989

Kinoshita, K. and Y. Myozyo (1974), Prog. Theor. Phys. 52, 6

Kinoshita, K. et al. (1974), Contributed Paper to XVII Int. Conference on High Energy Physics

Kiskis, J. (1974), SLAC-PUB-1477

Knapp, B. et al. (1975), Phys. Rev. Letters (to be published)

Krzywicki, A. (1964), Nuovo Cimento 32, 1067

_____ (1971a), Proc. of the Sixth Rencontre de Moriond

_____ (1971b), Nucl. Phys. B32, 149

Landau, L. D. (1953), Izu. An. SSSR, Ser. Fiz. 17, 51

Landshoff, P. V. (1974a), XVII Int. Conference on High Energy Physics, London

_____ (1974b), Phys. Rev. D 10, 1024

Landshoff, P. V. and J. C. Polkinghorne (1971), Nucl. Phys. B52, 541

_____ (1972a), Nucl. Phys. B53, 473

_____ (1972b), Phys. Reports 5C, 1

_____ (1973a), Phys. Letters 45B, 361

_____ (1973b), Phys. Rev. D 8, 927

_____ (1973c), Phys. Rev. D 8, 4157

_____ (1974), Phys. Rev. D 10, 891

Landshoff, P. V., J. C. Polkinghorne and R. Short (1971), Nucl. Phys. B28, 225

Lederman, L. (1975), preprint

Levin, E. M. and M. C. Ryskin (1973), Leningrad preprint 12

_____ (1974), Leningrad preprint 97

Lundby, A. (1973), in High Energy Collisions, edited by C. Quigg (American Institute of Physics, New York

Matveev, V. A., R. M. Muradyan and A. N. Tavkhelidze (1973), Lett. al Nuovo Cimento 7, 719

_____ (1974), JINR Report E2-8048

Meng Ta-Chung (1974), Phys. Rev. D 9, 3062

Menotti, P. (1974a), Phys. Rev. D 9, 2767

_____ (1974b), SLAC-PUB-1485

_____ (1975), Scuola Normale Superiore, Pisa preprint

Mueller-Kirsten, H. and G. Hite (1974), SLAC-PUB-1449

Newmeyer, J. L. and D. Sivers (1974), Phys. Rev. D 10, 1475

Nishijima, K. and M. Sato (1969), Prog. Theor. Phys. 42, 692

Orear, J. (1964), Phys. Rev. Letters 12, 112

Pearson, R. (1974), private communication

Pham, X. Y. and D. Wright (1974), SLAC-PUB-1516

Pokorski, S. and L. van Hove (1974a), CERN preprint TH-1565

_____ (1974b), CERN preprint TH-1930

Polkinghorne, J. C. (1972), Proc. of the Canadian Inst. of Particle Physics, McGill

_____ (1974), DAMTP 74/3

Preparata, G. (1974a), Nucl. Phys. B80, 299

_____ (1974b), CERN preprint TH. 1859

Raitio, R. and G. Ringland (1975), to be published as a SLAC preprint

Ramanauskas, A. et al. (1973), Phys. Rev. Letters 31, 1371

Ranft, G. (1974), CERN preprint

Roth, M. W. (1974), University of Illinois preprint ILL-TH-74-10

Rutherford, E. (1911), Philosophical Magazine 21, 669

Sachrajda, C. and R. Blankenbecler (1975), SLAC-PUB-1594

Sakai, S. (1973), Prog. Theor. Phys. 50, 1644

Savit, R. S. (1973), Ph.D. Thesis, SLAC-168

Schiff, L. (1970), Ann. Phys. (N.Y.) 63, 248

Schmidt, F. et al. (1973), Phys. Letters 45B, 157

Schmidt, M. (1974), Phys. Rev. D 9, 408

Schrempp, B. and F. Schrempp (1973), Nucl. Phys. B60, 110

Schrempp, B. and F. Schrempp (1975), Phys. Letters 55B, 303

Scott, D. M. (1973), Nuovo Cimento 18A, 271

Shei, S. S. (1974), Rockefeller University preprint

Sivers, D. (1975a), Ann. Phys. (N. Y.), to be published

_____ (1975b), Phys. Rev., to be published

Stack, J. (1967), Phys. Rev. 164, 1904

Sudakov, V. P. (1956), JETP 3, 65

Teper, M. (1974a), Phys. Letters 50B, 261

_____ (1974b), Westfield College preprint

Theis, W. (1972), Phys. Letters 42B, 246

Tiktopolos, G. (1974), UCLA preprint

Uematsu, T. (1974), Kyoto University preprint

Walker, J. K. (1973), in High Energy Collisions, edited by C. Quigg (American Institute of Physics, New York)

West, G. (1970), Phys. Rev. Letters 24, 1206

Wu, T. T. and C. N. Yang (1965), Phys. Rev. 137, B708

Yennie, D., S. Frautschi and H. Suura (1961), Ann. Phys. 13, 379

Yuta, H. et al. (1974), ANL preprint